THE STRESSES IN HYPERBOLIC PARABOLOID SHELLS USING THE MEMBRANE THEORY

by

Yousif Kellow Dawood

B.S., University of Baghdad, 1959

A MASTER'S REPORT

submitted in partial fulfillment of the

requirements for the degree

MASTER OF SCIENCE

Department of Civil Engineering

KANSAS STATE UNIVERSITY
Manhattan, Kansas

1965

Approved by:

V. A. Bosserman

Major Professor

TABLE OF CONTENTS

The Stresses in Hyperbolic Paraboloid Shells Using the Membrane Theory

by

Yousif K. Dawood

Synopsis

This paper includes a discussion of the limitations of the membrane theory. Definition and geometry of the hyperbolic paraboloid surface are discussed. The derivation of the partial differential equations of the stresses in doubly-curved structures is presented. Use of a stress function in calculating membrane stresses is given. Equations of stresses of some special cases are derived. A study of the economy and uses of these types of structures is made. The design of a hyperbolic paraboloidal groined vault is taken as an example.

INTRODUCTION

The Membrane Theory in many cases gives a clear insight into the stress distribution of doubly curved shells. It is a good by-pass to avoid the elaborate calculations encountered in using the bending theory.

Flügge[1] mentioned that shells which are egg-shaped or electric-bulb-shaped are much stronger than cylindrical ones. The two former can withstand remarkable forces without bending and without undergoing visible deformations. Therefore, the mechanism of the load-carrying capacity of such shells consists, essentially, of normal and shearing forces only.

Timoshenko[2] et al. stated that in many problems of shells the bending stresses can be neglected, and only stresses due to strain in the middle surface of the shells need to be considered. The doubly curved shells have been considered as examples of these problems where bending stresses have negligible effect.

Candela[3] said that equations of membrane stresses are sufficiently accurate to determine the stresses in doubly curved surfaces. That is because the deformations in such structures are very small. Flexure stresses are possible only if large deformations occur. However, bending stresses may be expected in some cases in the vicinity of the edge beams and at small zones near the supports.

---

[1]Wilhelm Flügge, Stress in Shells, Springer-Verlag, Berlin/Gottinge/Heidelberg, 1962, pp. 8-9.

[2]S. Timoshenko and S. Woinowsky-Kriegre, Theory of Plates and Shells, McGraw-Hill Book Company, Inc., 2nd Ed., 1959, pp. 432-465.

[3]Felix Candela, "Structure Application of Hyperbolic Paraboloidical Shells," ACI Journal, Jan. 1955, Vol. 26, No. 5, pp. 392.

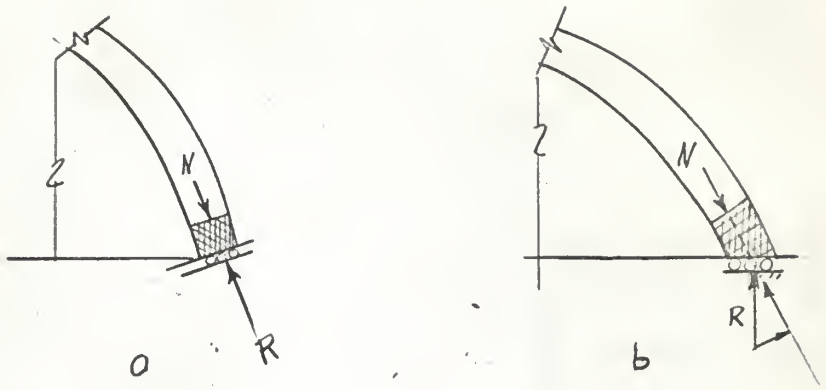

Fig. 1 - DEPENDENCE OF THE EQUILIBRIUM OF THE MEMBRANE FORCES ON THE BOUNDARY CONDITIONS.

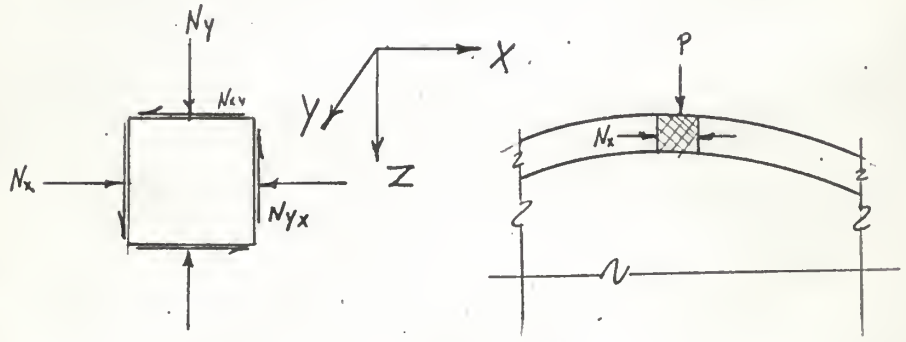

Fig. 2 - EQUILIBRIUM OF MEMBRANE FORCES UNDER A CONCENTRATED LOAD.

According to Parme[4], doubly curved concrete shells with edges stiffened by arches or ribs are so very strong because of their ability to carry any continuous load principally by direct stresses. He also mentioned the possibility of the occurrence of localized bending moments near the edges due to the effect of the displacement of the edge members, but for the most part the shells are free of flexural forces.

However, the justification of the membrane theory and its successes are closely connected with some factors which deserve careful study. These factors can be summarized as the boundary conditions, type of loading, and rise-to-span of shell ratio.

The effect of the boundary conditions on the membrane theory may be visualized by considering a simple example given by Pflüger[5]. In Fig. 1b only vertical reactions are possible, but the unit normal force "N" in the shell is acting in the direction of the meridien. Thus, the edge element cannot be in equilibrium because the reaction "R" produces a component that is normal to the middle surface and is not balanced by a counter force in the shell. The support shown in Fig. 1a would introduce reactions into the shell in accordance with the membrane theory.

The case of free edges was discussed by Candela[6]. He said that the existence of these free edges has a great effect on the internal stresses obtained by the membrane theory. Therefore, readjustment should be made of

---

[4]A. L. Parme, "Hyperbolic Paraboloid and Other Shells of Double Curvature," Proceedings of the ASCE-ST5, Vol. 28, Sept. 1956, pp. 1057/1-32.

[5]Alf Pflüger, Elementary Statics of Shells, English translation by Ervin Galanty, Dodge Corporation, N. Y., 2nd Ed., 1961, pp. 1-18, 91-93.

[6]F. Candela, "General Formulas for Membrane Stresses in Hyperbolic Paraboloidical Shells," ACI Journal, Vol. 32, No. 4, Oct. 1960, pp. 353-371.

the internal stresses. Such readjustment may disturb the condition of equilibrium in the shell. Accordingly, certain types of supports should be provided at the restrained edges which have the ability to absorb the non-balanced forces.

According to the above discussion, a general statement can be made: the membrane theory is applicable only if the boundary conditions are compatible with the conditions of equilibrium. However, results of tests on many hyperbolic paraboloid shells show a localized concentration of flexural stresses near the edge beams or rib stiffeners[7,8]. Therefore, special attention should be taken in the design of this part of the shells. Curves that show the secondary moment near the edge beams are presented by the Portland Cement Association[8].

The effect of the type of loading was discussed by Pflüger[5]. As shown in Fig. 2, assume the load is perpendicular to the middle surface, that is, in the direction of the Z-axis. The shell element on which the load is applied cannot possibly be in equilibrium. If the element were of infinitesimal magnitude, it would be conceivable to satisfy the conditions of equilibrium by assuming that N_x and N_y would produce components of sufficient magnitude to balance the load "P," because the curvature of the shell is in the direction of the concentrated load. Obviously then, concentrated loads normal to the middle surface are not compatible with the membrane theory. However, by a method analogous to that of the two-hinged parabolic arch, it can be proved that a uniformly distributed load will satisfy this condition[5].

---

[7]R. E. Rowe, "Test of Four Types of Hyperbolic Shells," Proceedings of the Symposium on Shell Research, Delft, Aug. 30-Sept. 2, 1961, pp. 16-35.

[8]Portland Cement Association, "Elementary Analysis of Hyperbolic Paraboloid Shells," 33 West Grand Avenue, Chicago 10, Ill. ST85.

The rise-to-span of shell ratio is one of the most important factors which may affect the validity of the membrane theory. The axial strain is the cause of the existence of the secondary bending moments[8]. For a moderate rise-to-span of shell ratio, the effect of axial strains is unimportant and can be safely ignored. However, when this ratio decreases, the effect of axial strains begins to exert a dominant influence on the behavior of the shell. The departure in behavior from that indicated by the membrane theory is analogous to that occurring in the two-hinged parabolic arch when it is subjected to uniform load with a decrease in the ratio of rise to span. In the parabolic arch, the horizontal component decreases as the ratio of rise to span decreases. With no rise the horizontal component decreases to zero, thus the secondary bending due to axial strains approaches the simple-beam bending moment. The Portland Cement Association suggests that when the rise-to-span of shell ratio is one-fifth or more, the effect of axial strains is unimportant and can be safely ignored. In other words, for such rise-to-span of shell ratio the bending moment has a negligible effect.

The hyperbolic paraboloids are shells of anticlastic doubly curved structures, that is, shells with negative curvature. These types of shells develop a state of stress favorable to the use of concrete. They show remarkable resistance to explosion, bombardment, earthquake and little sensitivity to foundation settlement[3]. They are economical due to their ruled surfaces which make them more easily formed by straight plank forms. Also, these shells give the architects a chance to depart from the conventional practice of beam and column buildings to more imaginative and graceful shapes of structures. Therefore, they are widely favored today.

The scope of this paper includes the description of the surface of the

hyperbolic paraboloid, the derivation of the general membrane stress equations, development of stress equations for some special cases, discussion of the boundary conditions and a sample design. A design of the Groined Vault using the membrane theory and in accordance with the Candela[6] Method will be presented as an example. The economic aspects of the hyperbolic paraboloid shells will also be discussed.

Surface Definition and Geometry

The hyperbolic paraboloid surface can be defined as a surface of translation or as a warped parallelogram. The surface of translation is formed by moving a vertical parabola, opened upward, over another vertical parabola opened downward as in Fig. 3b.

The warped parallelogram is formed by moving a straight line, always parallel to the XOZ plane (Fig. 3a) along the two straight, nonparallel, nonintersecting lines, the Y-axis and line ABC. The resulting surface is represented in Fig. 3a by the grid lines h_n and i_n, which are provisionally named the generators. Every point on the surface may be considered to be the intersection of two such lines contained in the surface.

The equation of the surface in birectangular coordinates can be derived by considering the basic quadrant, HOB, shown in Fig. 4. In triangle HA'A

$$\frac{c}{h} = \frac{X}{a}$$

or

$$c = \frac{Xh}{a}.$$

Also, in triangle Ed'd

$$\frac{Z}{c} = \frac{Y}{b}.$$

From this

$$Z = \frac{Yc}{b} = \frac{Y}{b} \cdot \frac{Xh}{a}$$

and

$$Z = \frac{h}{ab} XY$$

$$= KXY. \quad \ldots\ldots\ldots\ldots\ldots\ldots\ldots 1$$

Equation 1 represents the simplest possible equation of the second degree

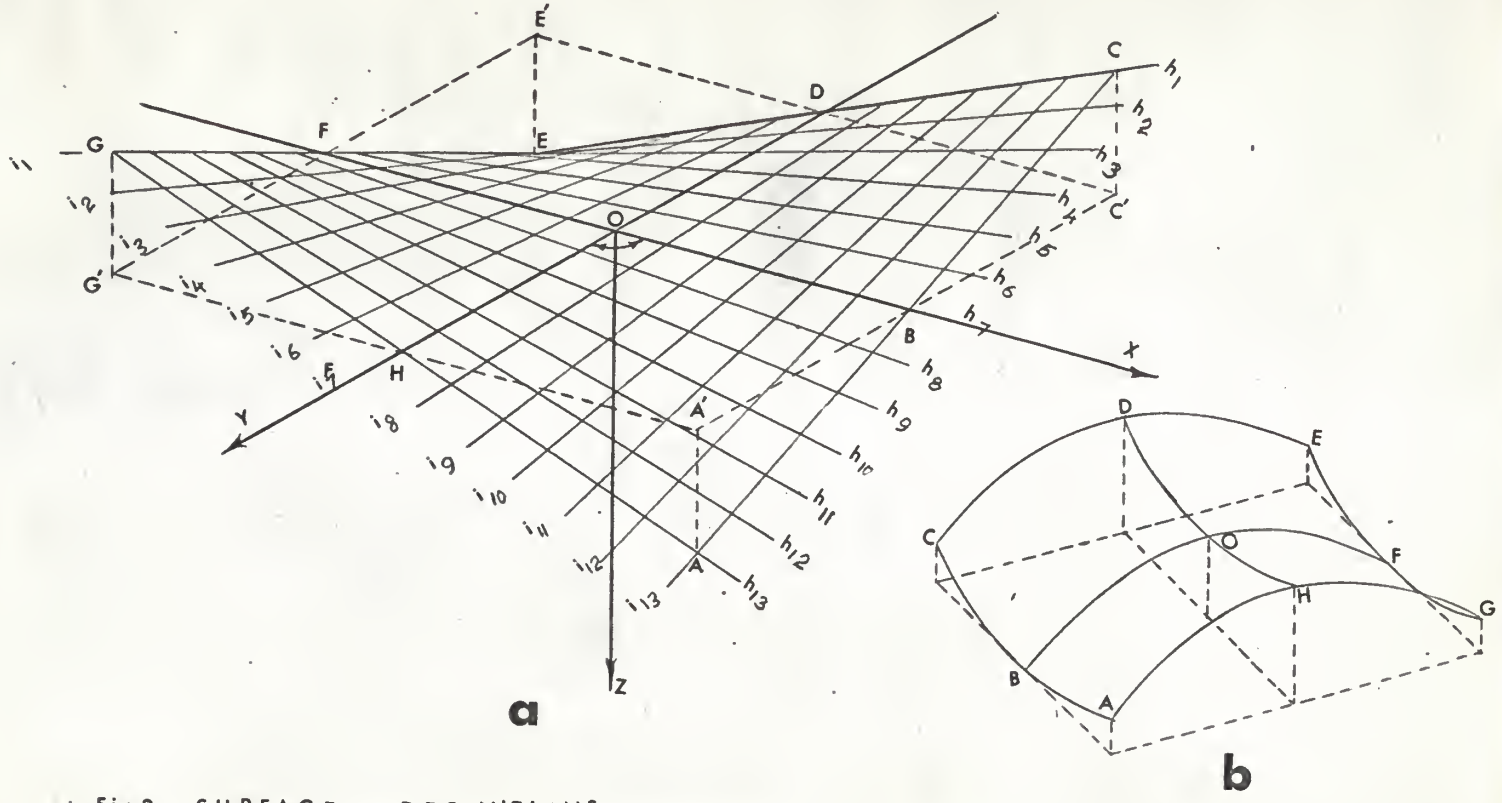

Fig.3– SURFACE DEFINITIONS

which describes the surface of the hyperbolic paraboloid.

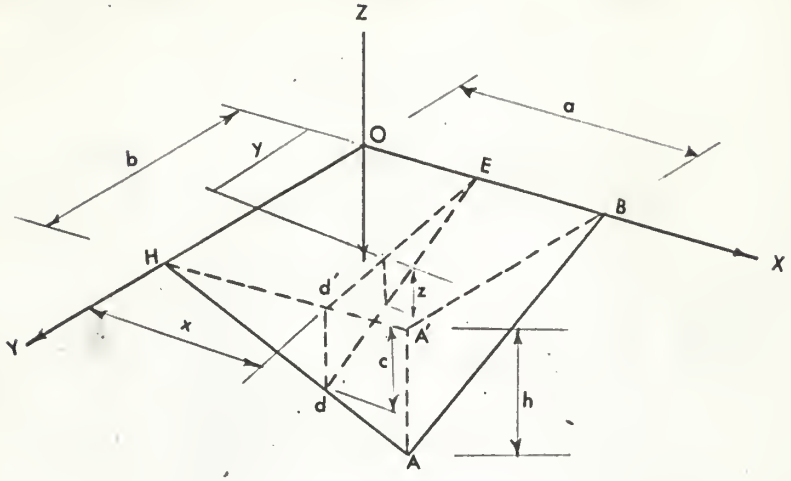

Fig.4 - GEOMETRY

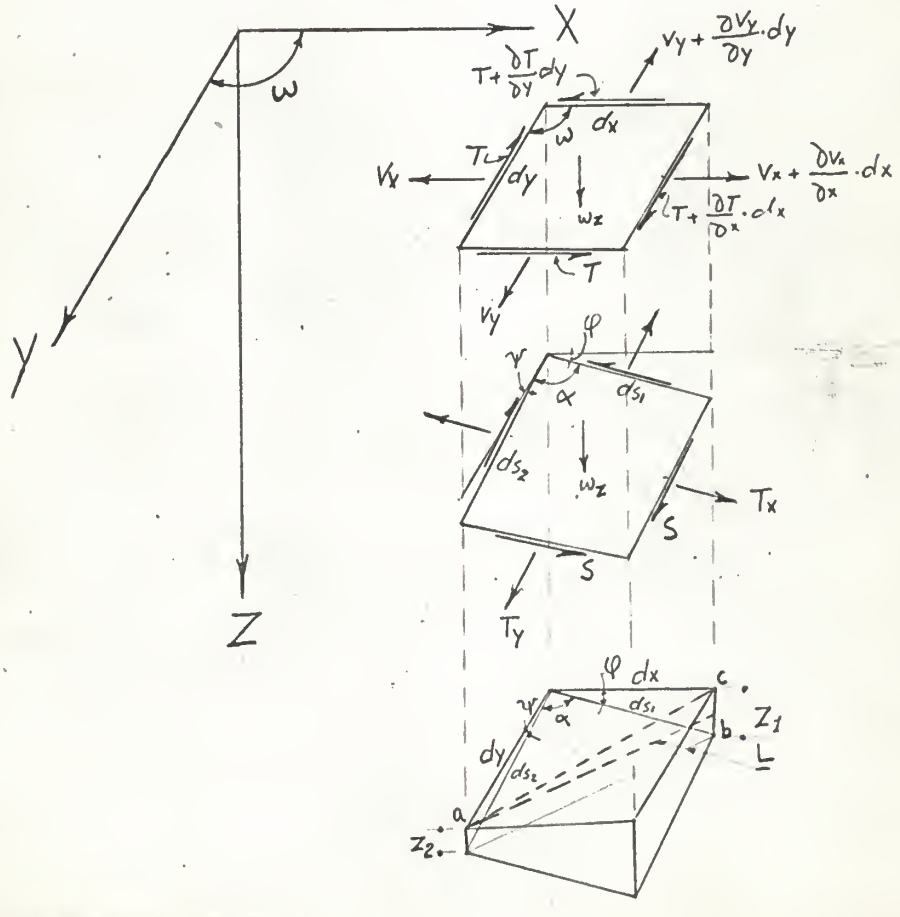

Fig.5 - MEMBRANE FORCES

Membrane Stresses for a Uniformly Distributed Surface Load

Fig. 5 shows a representative small element of a doubly curved shell formed by four intersecting generators. The direct stresses (stresses times the shell thickness), T_x and T_y measured in pounds per unit length, are positive when they create tension. The shearing stress, S, also measured in pounds per unit length, is positive when it creates tension in the diagonal direction of increasing values of X and Y. The load per unit of projected area, W_z, is considered positive when downward.

To simplify the expressions for equilibrium[9], the actual stresses are transformed into fictitious stresses acting on the projected area of the upper element in Fig. 5.

From geometry

$$ds_1 \cos \varphi = dx \quad \ldots\ldots\ldots\ldots \quad 2$$

and

$$ds_2 \cos \psi = dy. \quad \ldots\ldots\ldots\ldots \quad 3$$

The horizontal component of the normal stresses, T_x, is

$$T_x \cos \varphi \, ds_2 = T_x \frac{\cos \varphi}{\cos \psi} dy.$$

In order for the projected element to have the same total stress as the actual one

$$V_x \, dy = T_x \frac{\cos \varphi}{\cos \psi} dy$$

or

---

[9]K. W. Johansen, Stress Conditions in Shells Neglecting Bending, Copenhagen, Dansk Selskab for Bygningsstetik, Bygningsstatiske Meddelesler, 1938, pp. 61-84.

$$V_x = T_x \frac{\cos\varphi}{\cos\psi} \quad \ldots\ldots\ldots\ldots\ldots\ldots 4$$

By a similar procedure one can show that

$$V_y = T_y \frac{\cos\psi}{\cos\varphi} \quad \ldots\ldots\ldots\ldots\ldots\ldots 5$$

Using trigonometry it can be proved that

$$V_x = T_x \frac{\cos\varphi}{\cos\psi} = T_x \frac{\sec\psi}{\sec\varphi} = T_x \sqrt{\frac{1+\tan^2\psi}{1+\tan^2\varphi}}$$

But

$$\tan\varphi = \frac{\partial Z}{\partial X}$$

and

$$\tan\psi = \frac{\partial Z}{\partial Y}.$$

From Eq. 1

$$\frac{\partial Z}{\partial X} = KY$$

and

$$\frac{\partial Z}{\partial Y} = KX.$$

Therefore,

$$V_x = T_x \sqrt{\frac{1+K^2X^2}{1+K^2Y^2}} \quad \ldots\ldots\ldots\ldots 6$$

In a similar manner

$$V_y = T_y \sqrt{\frac{1+K^2Y^2}{1+K^2X^2}} \quad \ldots\ldots\ldots\ldots 7$$

Since,

$$S\cos\varphi ds_1 = Td_x$$

and by equation 2

$$ds_1 = \frac{dX}{\cos\varphi},$$

therefore,

$$S = T. \quad \ldots\ldots\ldots\ldots\ldots\ldots \quad 8$$

The equilibrium of stresses per unit length acting on the fictitious element along the Y-axis, considering the variation of the forces from the near end to the far end, and assuming only vertical load on the shells, yields:

$$\frac{\partial V_X}{\partial X} + \frac{\partial T}{\partial Y} = 0. \quad \ldots\ldots\ldots\ldots\ldots\ldots 9$$

Similarly, equilibrium along the X-axis gives

$$\frac{\partial V_Y}{\partial Y} + \frac{\partial T}{\partial X} = 0. \quad \ldots\ldots\ldots\ldots\ldots\ldots 10$$

The vertical components along the Z-axis are as follows:

The vertical component of the normal stress T_X is equal to $T_X \sin\varphi\, ds_2$. Substituting the values for T_X and ds_2 as given by Eqs. 3 and 4 gives

$$V_X \frac{\sin\varphi}{\cos\varphi} d_y = V_X \tan\varphi\, d_y = V_X \frac{\partial Z}{\partial X} d_y.$$

Therefore, the vertical component of T_X per unit length along the Y-axis is

$$V_X \frac{\partial Z}{\partial X}.$$

Similarly, the vertical component of T_Y per unit of length along the X-axis is

$$V_Y \frac{\partial Z}{\partial Y}.$$

The vertical component of the shear stress along the Y-axis is

$$S\, ds_2 \sin\psi = T \frac{\partial Z}{\partial Y} d_y$$

which per unit of length becomes

$$T\frac{\partial Z}{\partial Y}.$$

Similarly, the vertical component of shear along the X-axis is

$$T\frac{\partial Z}{\partial X}.$$

Considering the variation in the magnitude of stresses from one end to another, the summation of stresses in the Z-direction becomes

$$\frac{\partial}{\partial X}\left(V_X\frac{\partial Z}{\partial X}\right)+\frac{\partial}{\partial Y}\left(V_y\frac{\partial Z}{\partial Y}\right)+\frac{\partial}{\partial X}\left(T\frac{\partial Z}{\partial Y}\right)+\frac{\partial}{\partial Y}\left(T\frac{\partial Z}{\partial X}\right)=-W_z\sin w.$$

Differentiating and collecting terms yields

$$\frac{\partial Z}{\partial X}\left(\frac{\partial V_x}{\partial X}+\frac{\partial T}{\partial Y}\right)+\frac{\partial Z}{\partial Y}\left(\frac{\partial V_y}{\partial Y}+\frac{\partial T}{\partial X}\right)+V_x\frac{\partial^2 Z}{\partial X^2}+V_y\frac{\partial^2 Z}{\partial Y^2}+2T\frac{\partial^2 Z}{\partial X\partial Y}=-W_z\sin w.$$

Substituting Eqs. 9 and 10 in the above equation yields

$$V_x\frac{\partial^2 Z}{\partial X^2}+V_y\frac{\partial^2 Z}{\partial Y^2}+2T\frac{\partial^2 Z}{\partial X\partial Y}=-W_z\sin w \quad \ldots\ldots\ldots \quad 11$$

The use of a stress function[3] defining all three stress components will facilitate the solution of the differential equation. This stress function, F(x,y), reduces the three simultaneous Eqs. 9, 10 and 11 to one equation, the compatibility equation, with only one unknown.

It may be seen that Eqs. 9 and 10 are identically satisfied by taking

$$V_x=\frac{\partial^2 F}{\partial Y^2},\ V_y=\frac{\partial^2 F}{\partial Y^2},\ \text{and}\ T=-\frac{\partial^2 F}{\partial X\partial Y}.$$

Eq. 11, therefore, may be reduced to

$$\frac{\partial^2 F}{\partial Y^2}\cdot\frac{\partial^2 Z}{\partial X^2}+\frac{\partial^2 F}{\partial X^2}\cdot\frac{\partial^2 Z}{\partial Y^2}-2\frac{\partial^2 F}{\partial X\partial Y}\cdot\frac{\partial^2 Z}{\partial X\partial Y}=-W\sin w. \quad \ldots \quad 12$$

The form of Eq. 12 is of great importance in finding the membrane stresses of some doubly curved shells where the algebraic solution of the differential equation is difficult and some numerical procedures may be used. However, in the case of the hyperbolic paraboloid shells, subjected to a uniform surface load or uniformly distributed load on a horizontal projection, direct integration is relatively simple.

From the equation of the surface of the hyperbolic paraboloid, Eq. 1, it can be shown that

$$Z = KXY, \frac{\partial Z}{\partial X} = KY, \frac{\partial Z}{\partial Y} = KX, \frac{\partial^2 Z}{\partial X \partial Y} = K, \frac{\partial^2 Z}{\partial X^2} = 0, \text{ and } \frac{\partial^2 Z}{\partial Y^2} = 0.$$

Substituting these values in Eq. 12 gives

$$-2K \frac{\partial^2 F}{\partial X \partial Y} = -W_z \sin w,$$

but

$$T = \frac{\partial^2 F}{\partial X \partial Y}.$$

Therefore,

$$T = \frac{W_z}{2K} \sin w. \quad \ldots\ldots\ldots\ldots\ldots \quad 13$$

For hyperbolic paraboloid shells having a great rise, the dead load cannot be considered uniformly distributed on the horizontal projected area. Therefore, an expression for the dead load at any point in terms of W_z should be derived.

Assuming W_c is the load per unit area at any point, then

$$W_z \, dx dy \sin w = W_c \, ds_1 ds_2 \sin \alpha. \quad \ldots\ldots \quad 14$$

From the lower part of Fig. 5, it can be seen that

$$(ds_1)^2 + (ds_2)^2 - 2ds_1 ds_2 \cos \alpha = l^2. \quad \ldots \quad 15$$

$Z_1 = \sin\varphi\, ds_1$, and $Z_2 = \sin\psi\, ds_2$, $Z_1 - Z_2 = \sin\psi\, ds_2 - \sin\varphi\, ds_1$.

From the triangle, abc, one obtains

$$L^2 = (\sin\psi\, ds_2 - \sin\varphi\, ds_1)^2 + (d_x)^2 + (d_y)^2 - 2\, d_x\, d_y \cos w. \quad \ldots 16$$

Equating Eq. 14 to 15 and simplifying, it is found that

$$\cos\alpha = \sin\psi \sin\varphi - \frac{d_x}{ds_1} \cdot \frac{d_y}{ds_2}$$

but

$$\frac{ds_1}{d_x} = \sec\varphi = \frac{\partial z}{\partial x} = \sqrt{1+K^2Y^2}. \quad \ldots 17$$

and

$$\frac{ds_2}{d_x} = \sec\psi = \frac{\partial z}{\partial y} = \sqrt{1+K^2X^2}. \quad \ldots 18$$

Therefore,

$$\cos\alpha = \frac{\tan\psi \tan\varphi - \cos w}{\sqrt{(1+K^2X^2)(1+K^2Y^2)}} = \frac{K^4X^2Y^2 - \cos w}{\sqrt{(1+K^2X^2)(1+K^2Y^2)}} \quad \ldots 19$$

$$= \sqrt{1-\sin^2}$$

Therefore,

$$\sin^2\alpha = \frac{1-(K^4X^2Y^2-\cos w)^2}{(1+K^2X^2)(1+K^2Y^2)} = \frac{1+K^2X^2+K^2Y^2-\cos^2 w-2K^2XY\cos w}{(1+K^2X^2)(1+K^2Y^2)}$$

and

$$\sin\alpha = \sqrt{\frac{\sin^2 w+K^2X^2+K^2Y^2-2K^2XY\cos w}{(1+K^2X^2)(1+K^2Y^2)}}. \quad \ldots 20$$

Substituting Eqs. 20, 17 and 18 into Eq. 14 gives

$$W_s \sin w = W_c \sqrt{\sin w+K^2Y^2+K^2X^2-2K^2XY\cos w} = W_c\sqrt{\varphi}. \quad \ldots 21$$

where

$$\varphi = \sin^2 w+K^2Y^2+K^2X^2-2K^2XY\cos w.$$

Finally, substituting Eq. 21 into Eq. 13 results in

$$T = \frac{W_c}{2K}\sqrt{\varphi} \quad \ldots\ldots\ldots\ldots\ldots\ldots \quad 22$$

Differentiating Eq. 22 with respect to X and Y, then substituting these differentials in Eqs. 9 and 10, and integrating the resulting expressions with respect to X and Y, the equations for V_x and V_y are obtained.

$$\frac{\partial T}{\partial X} = \frac{1W_c}{2K}\,\frac{2K^2X-2K^2Y\cos w}{2\sqrt{\varphi}} \quad \ldots\ldots\ldots\ldots \quad 23$$

$$\frac{\partial T}{\partial Y} = \frac{-1W_c}{2K}\,\frac{2K^2Y-2K^2X\cos w}{2\sqrt{\varphi}} \quad \ldots\ldots\ldots\ldots \quad 24$$

Then by substituting Eq. 24 in Eq. 9 the following can be obtained:

$$V_x = \frac{+W_c}{2K}\int \frac{2K^2Y-2K^2X\cos w\,dX}{\sqrt{\varphi}}$$

$$= \frac{+W_c}{2K}\int \frac{2K^2Y\sin^2 w+2K^2Y\cos^2 w-2K^2X\cos w\,dX}{2\sqrt{\varphi}}$$

$$= \frac{+W_c}{2K}\left[\int \frac{\cos w(2K^2Y\cos w-2K^2Y)}{\sqrt{\varphi}}\,dX+\int \frac{2K^2Y\sin^2 w}{\sqrt{\varphi}}\cdot\frac{1}{2}\,dX\right]$$

$$= \frac{-W_c}{2K}\cos w\sqrt{\varphi} + \frac{W_cK^2Y\sin^2 w}{2K}\cdot\frac{1}{K}\log\left[K^2X-K^2Y\cos w+K\sqrt{\varphi}\right]+f(Y).$$

However, f(Y) is a constant of integration which can have any value including zero.

Assuming for convenience that

$$f(Y) = -\log k\sin w\sqrt{1+K^2Y^2} + f_1(Y).$$

Therefore,

$$V_x = \frac{-W_c}{2K}\cos w\sqrt{\varphi} + \frac{W_c}{2}Y\sin^2 w\log\left[\frac{KX-KY\cos w+\sqrt{\varphi}}{\sin w\sqrt{1+K^2Y^2}}\right] + f_1(Y). \quad \ldots \quad 25$$

Analogously,

$$V_y = \frac{-w_c}{2K} \cos w\sqrt{\varphi} + \frac{w_c}{2} X \sin^2 w \log\left[\frac{KY - KX\cos w + \sqrt{\varphi}}{\sin w \sqrt{1+K^2X^2}}\right] + f_2(X). \quad . \quad 26$$

The arbitrary functions of integration, $f_1(Y)$ and $f_2(X)$, allow us to satisfy certain edge conditions.

The forms of Eqs. 25 and 26 can be simplified for some special cases of hyperbolic paraboloid shells. The most common simplifications are:

(a) the case of a rectangular hyperbolic paraboloid shell, i.e., w=90 deg.

$$T = \frac{w_c}{2K}\sqrt{\varphi}. \quad . \quad . \quad . \quad . \quad . \quad . \quad . \quad . \quad . \quad . \quad . \quad . \quad . \quad . \quad . \quad . \quad . \quad 27$$

$$V_x = \frac{w_c}{2} Y \log\left[\frac{KX + \sqrt{\varphi}}{\sqrt{1+K^2Y^2}}\right] + f_1(Y). \quad . \quad . \quad . \quad . \quad . \quad . \quad . \quad 28$$

$$V_y = \frac{w_c}{2} X \log\left[\frac{KY + \sqrt{\varphi}}{\sqrt{1+K^2Y^2}}\right] + f_2(X). \quad . \quad . \quad . \quad . \quad . \quad . \quad . \quad 29$$

(b) the case of the uniformly distributed load on a horizontal projection

$$T = \frac{w_c \sin w}{2K} = \text{constant}. \quad . \quad . \quad . \quad . \quad . \quad . \quad . \quad . \quad . \quad . \quad 30$$

$$V_x = f_1(Y). \quad . \quad . \quad . \quad . \quad . \quad . \quad . \quad . \quad . \quad . \quad . \quad . \quad . \quad . \quad . \quad . \quad . \quad 31$$

$$V_y = f_2(X). \quad . \quad . \quad . \quad . \quad . \quad . \quad . \quad . \quad . \quad . \quad . \quad . \quad . \quad . \quad . \quad . \quad . \quad 32$$

Economy and Uses of Hyperbolic Paraboloid Shells

Madsen and Biggs[10] stated that "The hyperbolic paraboloid umbrella concrete roof costs less, uses less than half as many columns, inherently has great strength, will result in lower maintenance cost and is firesafe." They agreed that Felix Candela[3] was right when he said, "This is the most economical thing we have found."

The economic aspects of this type of structure derives from the fact that it develops a state of stress favorable to concrete, so that thin sections are anticipated. In almost all the shells constructed, the sections used vary from two inches to four inches. Their ruled surfaces make them more easily formed by straight plank forms. In addition, any hyperbolic paraboloid (hyper)roof composed of multi-units of similar hyper allows the re-using of the same forms in constructing each unit of the structure, which lowers the overall cost. Therefore, there can no longer be any doubt that this type of construction is the most economical of all framing systems in the range of spans commonly used.

The hyperbolic paraboloid shells can be used as roofs, such as the umbrella and the groined vault roofs, or as footings for columns[3] which are usually constructed in the form of an inverted umbrella.

---

[10]Gordon Madsen and Dutton Biggs, "Building for Economy with Hyperbolic Paraboloids," ACI Journal, October, 1960, No. 4, V. 32, pp. 373-383.

Design of the Groined Vault

A groined vault square in plan, formed by the intersection of two hypers with vertical axes, is designed as an example (Fig. 6).

Dimensions:

Side of the square = 70.00 feet.

Height of the crown = 20.00 feet.

$$\frac{\gamma}{2} = \tan^{-1} \frac{17.5}{35} = \tan^{-1} \frac{1}{2}.$$

Therefore,

$$\frac{\gamma}{2} = 26 \text{ deg. } 34 \text{ minutes.}$$

Design Data:

f'c = 3000 psi.

fs = 20000 psi., deformed bars.

n = 9.

v = 60.00 psi.

Code:

The ACI code (ACI 318-63) and the recommendations of the ACI Committee 334[11] are used.

Procedure of Design:

Since the plan of the structure is a square, symmetry permits us to investigate only one-eighth of the structure, say the triangle 1-8-22-1 shown in Fig. 6c.

---

[11]ACI Committee 334, "Concrete Shell Structures-Practice and Commentary," ACI Journal, No. 9, V. 61, Sept. 1964, pp. 1091-1108.

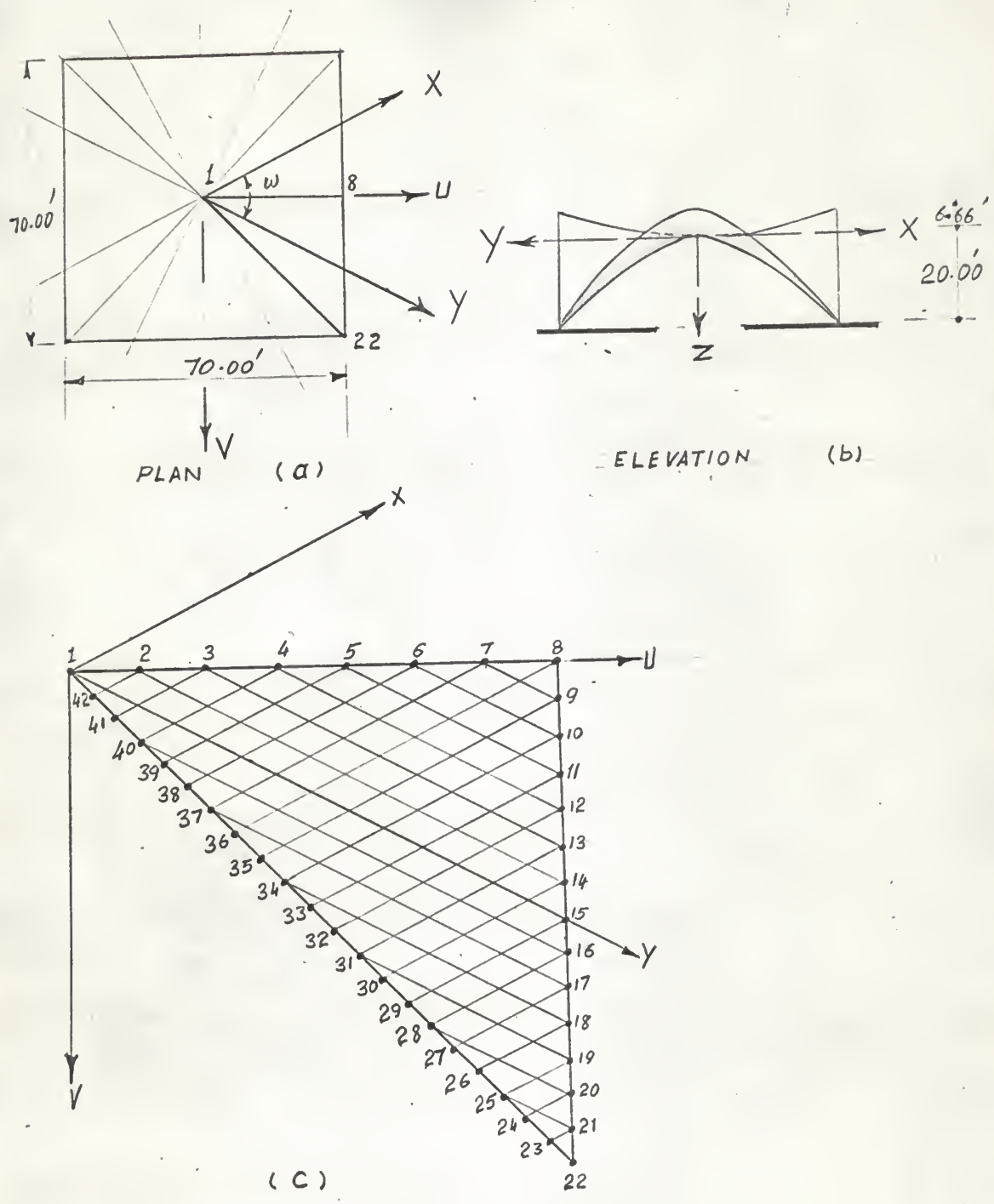

Fig.6-THE GROINED VAULT

The design procedure can be summarized by the following steps:

Step 1:

The coordinates of the boundary points 1 to 42 of the grid should be found. This may be accomplished easily by expressing the XY-coordinates in terms of rectangular coordinates. Referring to Fig. 7:

$$Y = \frac{n}{\sin \frac{w}{2}} \quad \ldots\ldots\ldots\ldots\ldots\ldots \quad 33$$

$$n = v - n = v - L \tan \frac{w}{2} \quad \ldots\ldots\ldots\ldots \quad 34$$

and,

$$\tan \frac{w}{2} = \frac{n}{L + U} \quad \ldots\ldots\ldots\ldots\ldots\ldots \quad 35$$

From Eqs. 33, 34 and 35, we obtain

$$Y = \frac{v + U \tan \frac{w}{2}}{2 \sin \frac{w}{2}} \quad \ldots\ldots\ldots\ldots\ldots\ldots \quad 36$$

Also,

$$\sin \frac{w}{2} = \frac{-n}{X} = \frac{-L}{\cos \frac{w}{2}} \quad \ldots\ldots\ldots\ldots\ldots \quad 37$$

From Eqs. 33, 34, 35, 36 and 37 it can be shown that

$$X = \frac{U \tan \frac{w}{2} - v}{2 \sin \frac{w}{2}} \quad \ldots\ldots\ldots\ldots\ldots\ldots \quad 38$$

Columns 1 and 2 of Table 1 show the values of X and Y of the boundary points 1 to 42 which are obtained by using Eqs. 36 and 38. In order to find the Z-values, the constant, K, of Eq. 1 should be computed.

$$K = \frac{Z_{22}}{X_{22} Y_{22}} = \frac{20}{-19.6 \times 58.7} = -0.0174.$$

Column 3 of Table 1 shows the values of Z.

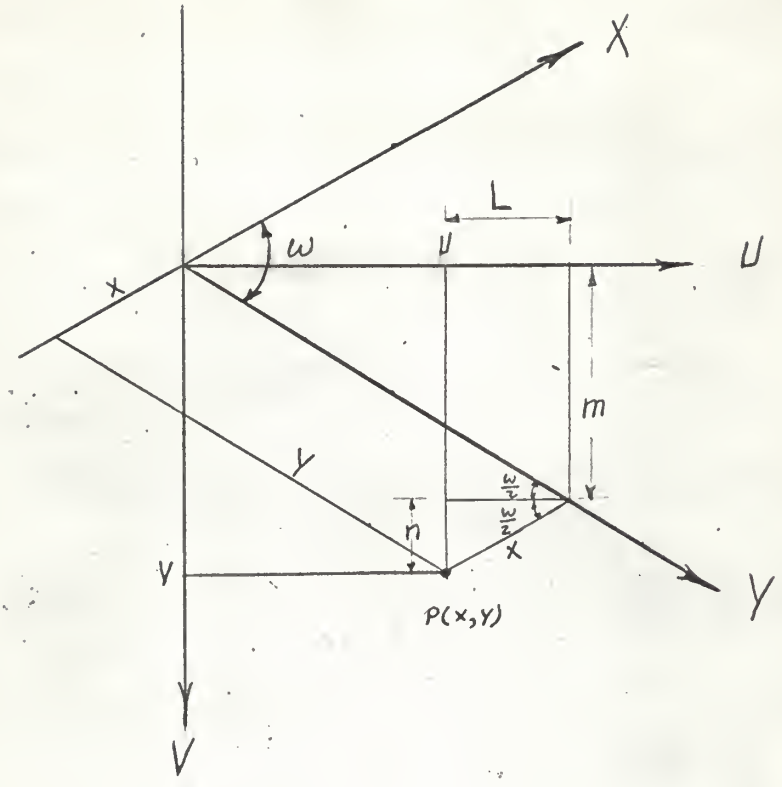

Fig. 7 – COORDINATES SYSTEM

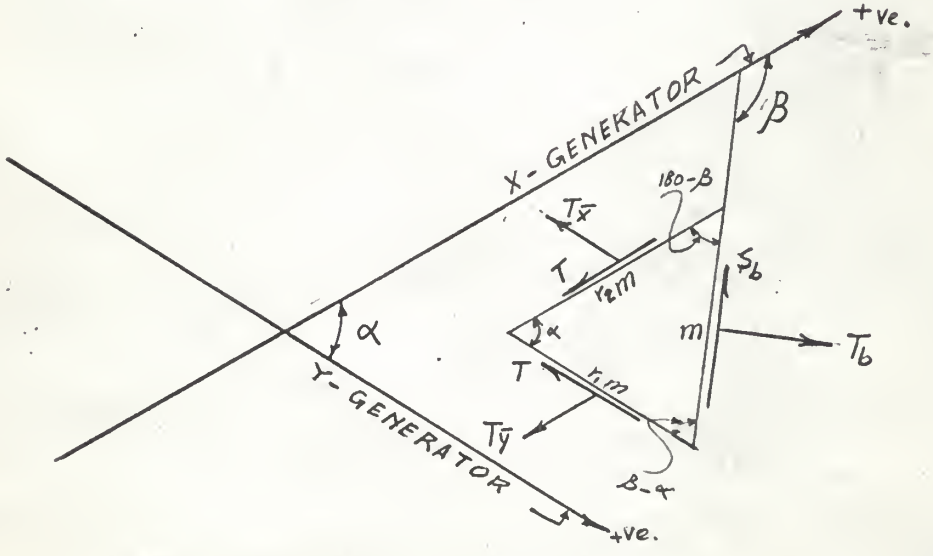

Fig. 8 – CONDITIONS OF EQUILBRIUM

Step 2:

The dead load on the basis of horizontal projection should be calculated. Assuming the thickness of the shell is three inches, then

D. L. = $\frac{3}{12}$ x 1 x 1 x 150 = 37.5 lb. per sq. ft.

Roofing = 12.5 lb. per sq. ft.[12]

Total D. L. = 50.0 lb. per sq. ft.

The dead load per unit length of edge is

2 x 50 = 100 lb. per ft.

= .1 K. per ft.

From Eqs. 22, 25, and 26, the basic values of T, V_x, and V_y are computed. To suit the tabulation representation, these equations may be put in more abridged form:

$$T = \frac{-1}{2K} W_c \sqrt{\varphi}$$

$$V_x = -T \cos w + A \log B + f_1(Y)$$

$$V_y = -T \cos w + C \log D + f_2(X)$$

where:

$$A = \frac{1}{2} W_c Y \sin^2 w$$

$$B = \frac{KX - KY \cos w + \sqrt{\varphi}}{\sin w \sqrt{1 + K^2 Y^2}}$$

$$C = \frac{1}{2} W_c X \sin^2 w$$

---

[12]Elwyn E. Seelye, Data Book for Civil Engineers, John Wiley and Sons, Inc. 3rd Edition, 1960, Vol. 1, pp. 1-09.

$$D = \frac{KY - KX \cos w + \sqrt{\varphi}}{\sin w \sqrt{1 + K^2 X^2}}.$$

The various items which are necessary for this step are shown in columns 4 to 34 of Table 1.

The boundary points in this step are treated as interior ones in which $f_1(Y)$ and $f_2(X)$ are assumed to be equal to zero. Determination of the exact values of these functions and readjustment of V_x and V_y is done in later steps.

Step 3:

The stresses S, T_x, and T_y shown in Fig. 5 are parallel to the generators. However, the stresses along the boundary need to be investigated. T_x and T_y are oblique stresses, so the usual constructions of Mohr's Circle cannot be used here. Fig. 8 shows the conditions of equilibrium of an element in the first quadrant formed by two intersecting generators and some arbitrary section which makes an angle β with the positive direction of the x-generator. From trigonometry it can be shown that

$$\frac{r_1 a}{\sin} = \frac{r_2 a}{\sin(\beta - \alpha)} = \frac{a}{\sin \alpha}.$$

From which is obtained

$$r_1 = \frac{\sin \beta}{\sin \alpha} \quad \text{and} \quad r_2 = \frac{\sin(\beta - \alpha)}{\sin \alpha}.$$

By multiplying S, T_x, and T_y by the corresponding length of the sides and resolving these forces in a direction normal and parallel to the section, the values of the normal and tangential stresses, T_b and S_b, are obtained.

$$T_b = T_x \frac{\sin^2 \beta}{\sin \alpha} + 2T \frac{\sin \beta \sin(\beta - \alpha)}{\sin \alpha} + T_y \frac{\sin^2(\beta - \alpha)}{\sin \alpha} \quad \ldots\ldots 39$$

$$S_b = -T_x \frac{\sin \beta \cos \beta}{\sin \alpha} - T \frac{\sin(2\beta - \alpha)}{\sin \alpha} - T_y \frac{\sin(\beta - \alpha)\cos(\beta - \alpha)}{\sin \alpha} \quad \ldots 40$$

Table 1. Basic values of stresses.

Point	$\frac{X}{1}$	$\frac{Y}{2}$	$\frac{Z}{3}$	$\frac{X^2}{4}$	$\frac{Y^2}{5}$	$\frac{K^2X^2}{6}$	$\frac{K^2Y^2}{7}$
1	0.0000	0.0000	0.0000	0.0000	0.0000	0.0000	0.0000
2	2.8000	2.8000	- 0.1363	7.8400	7.8400	0.0024	0.0024
3	5.6000	5.6000	- 0.5451	31.3600	31.3600	0.0095	0.0095
4	8.4000	8.4000	- 1.2266	70.5600	70.5600	0.0213	0.0213
5	11.2000	11.2000	- 2.1806	125.4400	125.4400	0.0379	0.0379
6	14.0000	14.0000	- 3.4071	196.0000	196.0000	0.0592	0.0592
7	16.8000	16.8000	- 4.9063	282.2400	282.2400	0.0853	0.0853
8	19.6000	19.6000	- 6.6780	384.1600	384.1600	0.1161	0.1161
9	16.8000	22.4000	- 6.5417	282.2400	501.7600	0.0853	0.1516
10	14.0000	25.2000	- 6.1329	196.0000	635.0400	0.0592	0.1919
11	11.2000	28.0000	- 5.4514	125.4400	784.0000	0.0379	0.2369
12	8.4000	30.8000	- 4.4974	70.5600	948.6400	0.0213	0.2867
13	5.6000	33.6000	- 3.2709	31.3600	1128.9600	0.0095	0.3411
14	2.8000	36.4000	- 1.7717	7.4800	1324.9600	0.0024	0.4004
15	0.0000	39.2000	0.0000	0.0000	1536.6400	0.0000	0.4643
16	- 2.8000	42.0000	2.0443	7.4800	1764.0000	0.0024	0.5330
17	- 5.6000	44.8000	4.3611	31.3600	2007.0400	0.0095	0.6065
18	- 8.4000	47.6000	6.9506	70.5600	2265.7600	0.0213	0.6847
19	-11.2000	50.4000	9.8126	125.4400	2540.1600	0.0379	0.7676
20	-14.0000	53.2000	12.9472	196.0000	2830.2400	0.0592	0.8550
21	-16.8000	56.0000	16.3543	282.2400	3136.0000	0.0853	0.9476
22	-19.6000	58.8000	20.0000	384.1600	3457.4400	0.1161	1.1608
23	-18.7000	56.0000	18.2044	349.6900	3136.0000	0.1057	0.9476
24	-17.7800	53.2000	16.4430	316.8400	2830.0000	0.0957	0.8550
25	-16.8000	50.0400	14.7184	282.2400	2540.1600	0.0853	0.7676
26	-15.8800	47.6000	13.1381	252.8000	2265.7600	0.0764	0.6847
27	-14.8500	44.8000	11.5651	220.5200	2007.0400	0.0666	0.6065
28	-14.0200	42.0000	10.2360	196.5800	1764.0000	0.0594	0.5330
29	-13.0800	39.2000	8.9127	171.0900	1536.6400	0.0517	0.4643
30	-12.1800	36.4000	7.7069	148.3500	1324.9600	0.0448	0.4004
31	-11.2700	33.6000	6.5828	127.0700	1128.9600	0.0384	0.3411
32	-10.3000	30.8000	5.5146	106.0900	948.6400	0.0321	0.2867
33	- 9.3600	28.0000	4.5555	87.6100	784.0000	0.0265	0.2369
34	- 8.4500	25.2000	3.7019	71.4000	635.0400	0.0216	0.1919
35	- 7.5100	22.4000	2.9244	56.4000	501.7600	0.0170	0.1516
36	- 6.5800	19.6000	2.2419	43.3000	384.1600	0.0131	0.1161
37	- 5.6400	16.8000	1.6559	31.8100	282.2400	0.0096	0.0853
38	- 4.7200	14.0000	1.1488	22.2800	196.0000	0.0067	0.0592
39	- 3.7700	11.2000	0.7362	14.2100	125.4400	0.0043	0.0379
40	- 2.8400	8.4000	0.4146	8.0700	70.5600	0.0024	0.0213
41	- 1.9100	5.6000	0.1858	3.6500	31.3600	0.0011	0.0095
42	- 0.9300	2.8000	0.0453	0.8600	7.8400	0.0003	0.0024

Table 1. (Cont.)

Point	XY 8	KX 9	KY 10	K^2XY 11	KX cos w 12	KY cos w 13	$2K^2XY$ cos w 14
1	0.0000	0.0000	0.0000	0.0000	0.0000	0.0000	0.0000
2	7.8400	-0.0487	-0.0487	0.0024	-0.0292	-0.0292	0.0029
3	31.3600	-0.0973	-0.0973	0.0095	-0.0584	-0.0584	0.0114
4	70.5600	-0.1460	-0.1460	0.0213	-0.0876	-0.0876	0.0256
5	125.4400	-0.1947	-0.1947	0.0379	-0.1168	-0.1168	0.0455
6	196.0000	-0.2434	-0.2434	0.0592	-0.1460	-0.1460	0.0710
7	282.2400	-0.2920	-0.2920	0.0853	-0.1752	-0.1752	0.1023
8	384.1600	-0.3407	-0.3407	0.1161	-0.2044	-0.2044	0.1393
9	376.3200	-0.2920	-0.3894	0.1137	-0.1752	-0.2336	0.1364
10	352.8000	-0.2434	-0.4381	0.1066	-0.1460	-0.2628	0.1279
11	313.6000	-0.1947	-0.4867	0.0948	-0.1168	-0.2920	0.1017
12	258.7200	-0.1460	-0.5354	0.0782	-0.0876	-0.3212	0.0938
13	188.1600	-0.0973	-0.5841	0.0568	-0.0584	-0.3504	0.0681
14	101.9200	-0.0487	-0.6327	0.0308	-0.0292	-0.3796	0.0370
15	0.0000	0.0000	-0.6814	0.0000	0.0000	-0.4088	0.0000
16	-117.6000	0.0487	-0.7301	-0.0355	0.0292	-0.4380	-0.0426
17	-250.8800	0.0973	-0.7788	-0.0758	0.0584	-0.4672	-0.0909
18	-399.8400	0.1460	-0.8274	-0.1208	0.0876	-0.4964	-0.1449
19	-564.4800	0.1947	-0.8761	-0.1706	0.1168	-0.5256	-0.2047
20	-744.8000	0.2434	-0.9248	-0.2251	0.1460	-0.5548	-0.2701
21	-940.8000	0.2920	-0.9735	-0.2843	0.1752	-0.5841	-0.3411
22	-1152.4800	0.3407	-1.0221	-0.3483	0.2044	-0.6132	-0.4179
23	-1047.2000	0.3251	-0.9735	-0.3164	0.1950	-0.5841	-0.3764
24	-948.5600	0.3091	-0.9248	-0.2866	0.1854	-0.5548	-0.3439
25	-840.6700	0.2920	-0.8761	-0.2540	0.1752	-0.5256	-0.3048
26	-756.6800	0.2760	-0.8274	-0.2286	0.1656	-0.4964	-0.2743
27	-665.2800	0.2581	-0.7788	-0.2010	0.1548	-0.4672	-0.2412
28	-588.8400	0.2437	-0.7301	-0.1779	0.1462	-0.4380	-0.2135
29	-513.7800	0.2274	-0.6814	-0.1552	0.1364	-0.4088	-0.1862
30	-443.3500	0.2117	-0.6327	-0.1340	0.1270	-0.3796	-0.1608
31	-380.7000	0.1959	-0.5841	-0.1150	0.1175	-0.3504	-0.1380
32	-319.3000	0.1790	-0.5354	-0.0965	0.1074	-0.3212	-0.1158
33	-263.7600	0.1627	-0.4867	-0.0797	0.0976	-0.2920	-0.0956
34	-214.4600	0.1469	-0.4381	-0.0648	0.0881	-0.2628	-0.0777
35	-169.5700	0.1305	-0.3894	-0.0512	0.0783	-0.2336	-0.0614
36	-129.9500	0.1143	-0.3407	-0.0393	0.0688	-0.2044	-0.0471
37	- 95.0300	0.0980	-0.2920	-0.0287	0.0588	-0.1752	-0.0344
38	- 66.9300	0.0820	-0.2434	-0.0202	0.0492	-0.1460	-0.0242
39	- 42.6800	0.0655	-0.1947	-0.0129	0.0393	-0.1168	-0.0155
40	- 24.2500	0.0494	-0.1460	-0.0073	0.0296	-0.0876	-0.0087
41	- 10.9600	0.0332	-0.0973	-0.0033	0.0199	-0.0584	-0.0040
42	- 2.6000	0.0162	-0.0487	-0.0007	0.0097	-0.0292	-0.0008

Table 1. (Cont.)

Point	15	$1+K^2X^2$ 16	$1+K^2Y^2$ 17	sin w $1+K^2X^2$ 18	sin w $1+K^2Y^2$ 19	cos w 20	$\sum_{X}^{Z} \sin^2 w$ 21
1	0.8000	1.0000	1.0000	0.8000	0.8000	0.4800	0.0000
2	0.8020	1.0020	1.0020	0.8016	0.8016	0.4812	0.8960
3	0.8050	1.0040	1.0040	0.8032	0.8032	0.4829	1.7920
4	0.8110	1.0100	1.0100	0.8080	0.8080	0.4866	2.6880
5	0.8180	1.0150	1.0150	0.8120	0.8120	0.4908	3.5840
6	0.8300	1.0290	1.0290	0.8232	0.8232	0.4980	4.4800
7	0.8420	1.0410	1.0410	0.8328	0.8328	0.5158	5.3760
8	0.8500	1.0550	1.0550	0.8524	0.8524	0.5136	6.2720
9	0.8600	1.0410	1.0710	0.8238	0.8408	0.5160	5.3760
10	0.8740	1.0290	1.0950	0.8232	0.8440	0.5244	4.4800
11	0.9020	1.0150	1.1100	0.8120	0.8880	0.5411	3.5840
12	0.9290	1.0100	1.1320	0.8080	0.9356	0.5573	2.6880
13	0.9600	1.0040	1.1580	0.8032	0.9264	0.5759	1.7920
14	1.0000	1.0020	1.1810	0.8016	0.9448	0.6000	0.8960
15	1.0500	1.0000	1.2090	0.8000	0.9672	0.6299	0.0000
16	1.1000	1.0020	1.2350	0.8016	0.9880	0.6599	-0.8960
17	1.1610	1.0040	1.2630	0.8032	1.0104	0.6965	-1.7920
18	1.2210	1.0100	1.2990	0.8080	1.0392	0.7325	-2.6880
19	1.2850	1.0150	1.3300	0.8120	1.0640	0.7709	-3.5840
20	1.3500	1.0290	1.3600	0.8232	1.0880	0.8099	-4.4800
21	1.4150	1.0410	1.3950	0.8328	1.1160	0.8489	-5.3760
22	1.4460	1.0780	1.4720	0.8524	1.1936	0.8675	-6.2720
23	1.4330	1.0490	1.3950	0.8392	1.1160	0.8627	-5.9840
24	1.3560	1.0450	1.3600	0.8360	1.0880	0.8135	-5.6896
25	1.3360	1.0410	1.3300	0.8328	0.0640	0.8015	-5.3760
26	1.2940	1.0350	1.2990	0.8280	1.0392	0.7763	-5.0816
27	1.2440	1.0330	1.2630	0.8264	1.0104	0.7463	-4.7520
28	1.2010	1.0280	1.2350	0.8224	0.9880	0.7205	-4.4864
29	1.1590	1.0230	1.2090	0.8184	0.9672	0.6953	-4.1856
30	1.1160	1.0200	1.1810	0.8160	0.9448	0.6695	-3.8976
31	1.0760	1.0180	1.1580	0.8144	0.9264	0.6455	-3.6064
32	1.0370	1.0150	1.1320	0.8120	0.9356	0.6221	-3.2960
33	0.9760	1.0120	1.1100	0.8096	0.8880	0.5855	-2.9952
34	0.9660	1.0100	1.0950	0.8080	0.8440	0.5795	-2.7040
35	0.9340	1.0070	1.0710	0.8056	0.8408	0.5603	-2.4032
36	0.9040	1.0040	1.0550	0.8032	0.8524	0.5423	-2.1056
37	0.8770	1.0030	1.0410	0.8024	0.8320	0.5262	-1.8048
38	0.8560	1.0020	1.0290	0.8016	0.8232	0.5136	-1.5104
39	0.8360	1.0010	1.0150	0.8008	0.8120	0.5016	-1.2064
40	0.8200	1.0000	1.0100	0.8000	0.8080	0.4920	-0.9088
41	0.8090	1.0000	1.0040	0.8000	0.8032	0.4854	-0.6112
42	0.8030	1.0000	1.0020	0.8000	0.8016	0.4818	-0.2976

Table 1. (Cont.)

Point	$\frac{Y}{2}\sin^2 w$ / 22	A / 23	B / 24	C / 25	D / 26	log B / 27	log D / 28
1	0.0000	0.0000	1.0000	0.0000	1.0000	0.0000	0.0000
2	0.8960	0.0896	0.9761	0.0896	0.9761	-0.0243	-0.0243
3	1.7920	0.1792	0.9538	0.1792	0.9538	-0.0471	-0.0471
4	2.6880	0.2688	0.9314	0.2688	0.9314	-0.0710	-0.0710
5	3.5840	0.3584	0.9114	0.3584	0.9114	-0.0932	-0.0932
6	4.4800	0.4480	0.8911	0.4480	0.8911	-0.1154	-0.1154
7	5.3760	0.5376	0.8708	0.5376	0.8708	-0.1383	-0.1383
8	6.2720	0.6272	0.8443	0.6272	0.8443	-0.1707	-0.1707
9	7.1680	0.7168	0.9534	0.5376	0.7839	-0.0481	-0.2433
10	8.0640	0.8064	1.0585	0.4480	0.7069	0.0582	-0.3467
11	8.9600	0.8960	1.1253	0.3584	0.6553	0.1088	-0.4231
12	9.8650	0.9865	1.1802	0.2688	0.5955	0.1655	-0.5184
13	10.7520	1.0752	1.3095	0.1792	0.5407	0.2700	-0.6149
14	11.6480	1.1648	1.4086	0.0896	0.4946	0.3436	-0.7032
15	12.5440	1.2544	1.5083	0.0000	0.3999	0.4121	-0.9163
16	13.4400	1.3440	1.6060	-0.0896	0.4250	0.4731	-0.8557
17	14.3360	1.4336	1.8285	-0.1792	0.4031	0.6003	-0.9088
18	15.2320	1.5232	1.7065	-0.2688	0.3787	0.5344	-0.9702
19	16.1280	1.6128	1.8847	-0.3584	0.3597	0.6337	-1.0217
20	17.0240	1.7024	1.9744	-0.4480	0.3392	0.6805	-1.0817
21	17.9200	1.7920	2.0530	-0.5376	0.3198	0.7193	-1.1394
22	18.8160	1.8816	2.0106	-0.6272	0.2575	0.6936	-1.3567
23	17.9200	1.7920	2.1032	-0.5984	0.3211	0.6981	-1.1305
24	17.0240	1.7024	2.2256	-0.5689	0.3309	0.7990	-1.2347
25	16.1280	1.6128	2.0343	-0.5376	0.3493	0.7102	-1.0526
26	15.2320	1.5232	1.9931	-0.5082	0.5961	0.6881	-1.0147
27	14.3360	1.4336	1.9488	-0.4752	0.5714	0.6678	-0.9795
28	13.4400	1.3440	1.9009	-0.4486	0.6418	0.6418	-0.9288
29	12.5440	1.2544	1.8538	-0.4186	0.6153	0.6153	-0.8734
30	11.6480	1.1648	1.8070	-0.3898	0.5913	0.5913	-0.8285
31	10.7520	1.0752	1.7654	-0.3606	0.6231	0.5678	-0.7853
32	9.8650	0.9865	1.6958	-0.3296	0.5306	0.5306	-0.7318
33	8.9600	0.8960	1.6104	-0.2995	0.4762	0.4762	-0.7339
34	8.8064	0.8806	1.5798	-0.2704	0.4574	0.4574	-0.6152
35	7.1680	0.7168	1.5173	-0.2403	0.4187	0.4187	-0.5534
36	6.2720	0.6272	1.4157	-0.2106	0.3471	0.3471	-0.4894
37	5.3760	0.5376	1.3830	-0.1805	0.3241	0.3241	-0.4232
38	4.4800	0.4480	1.3178	-0.1510	0.2752	0.2752	-0.3581
39	3.5480	0.3548	1.2520	-0.1206	0.2245	0.2245	-0.2890
40	2.6880	0.2688	1.1861	-0.0909	0.1697	0.1697	-0.2200
41	1.7920	0.1792	1.1242	-0.0611	0.1129	0.1129	-0.1491
42	0.8960	0.0896	1.0459	-0.0298	0.0438	0.0438	-0.0693

Table 1. (Concl.)

Point	A log B	C log D	T k/ft.	T cos w	VX k/ft.	VY k/ft.
	29	30	31	32	33	34
1	0.0000	0.0000	2.2966	1.3793	1.3793	1.3793
2	-0.0022	-0.0022	2.3018	1.3811	1.3789	1.3789
3	-0.0085	-0.0085	2.3102	1.3861	1.3776	1.3776
4	-0.0191	-0.0191	2.3268	1.3973	1.3782	1.3782
5	-0.0358	-0.0358	2.3449	1.4069	1.3711	1.3711
6	-0.0516	-0.0516	2.3635	1.4301	1.3785	1.3785
7	-0.0744	-0.0744	2.4166	1.4512	1.3768	1.3768
8	-0.1071	-0.1071	2.4600	1.4760	1.3689	1.3689
9	-0.0344	-0.1302	2.4658	1.4795	1.4451	1.3493
10	0.0388	-0.1554	2.5160	1.5108	1.5496	1.3554
11	0.0975	-0.1512	2.5898	1.5539	1.6514	1.4027
12	0.1635	-0.1393	2.6610	1.5966	1.7601	1.4573
13	0.2905	-0.1102	2.7587	1.6552	1.9457	1.5450
14	0.4000	-0.0628	2.8735	1.7241	2.1241	1.6613
15	0.5160	0.0000	3.0189	1.8113	2.3273	1.8113
16	0.6351	0.0767	3.1600	1.8960	2.5311	1.9727
17	0.8611	0.1629	3.3401	1.9041	2.7652	2.0680
18	0.8100	0.2618	3.5011	2.1007	2.9107	2.3625
19	1.0196	0.3660	3.6859	2.2139	3.2335	2.5799
20	1.1585	0.4850	3.8788	2.3273	3.4858	2.8123
21	1.2810	0.6221	4.0654	2.4392	3.7202	3.0613
22	1.3045	0.8518	4.1500	2.4900	3.7945	3.3418
23	1.2511	0.6686	4.1354	2.4812	3.7323	3.1498
24	1.3605	0.7018	3.8897	2.3338	3.6943	3.0356
25	1.1484	0.5655	3.8369	2.3021	3.4505	2.8676
26	1.0499	0.5160	3.7210	2.2326	3.2825	2.7486
27	0.9599	0.4659	3.5789	2.1473	3.1072	2.6132
28	0.8643	0.4166	3.4500	2.0700	2.9343	2.4866
29	0.7718	0.3658	3.3253	1.9952	2.7670	2.3610
30	0.6900	0.3229	3.3300	1.9980	2.6880	2.3209
31	0.6182	0.2828	3.0855	1.8513	2.4695	2.1341
32	0.5235	0.2418	2.9797	1.7878	2.3113	2.0296
33	0.4267	0.2195	2.8000	1.6800	2.1067	1.8995
34	0.4035	0.1661	2.7689	1.6613	2.0648	1.8374
35	0.3000	0.1338	2.6795	1.6077	1.9077	1.7415
36	0.2810	0.1029	2.5942	1.5565	1.8375	1.6594
37	0.1731	0.0754	2.5181	1.5109	1.6840	1.5863
38	0.1234	0.0542	2.4579	1.4747	1.5981	1.5289
39	0.0796	0.0349	2.4000	1.4400	1.5196	1.4749
40	0.0456	0.0200	2.3500	1.4100	1.4556	1.4300
41	0.0203	0.0091	2.3199	1.3919	1.4122	1.4010
42	0.0039	0.0023	2.3000	1.3800	1.3839	1.3823

Values of angle β may be obtained by a method analogous to that used in obtaining angle α of Eq. 19.

Therefore,

$$\cos \beta = \frac{KY\, q_b + \cos w_b}{\sqrt{(1+K^2Y^2)\,(1+q_b^2)}} \quad \ldots\ldots\ldots 41$$

where

w_b is the projection of angle β on the XY-plane.

q_b is the trigonometrical tangent of the angle formed by the straight line representing the section with the XY-plane, i. e.,

$$q_b = \frac{Z_i - Z_j + 1}{c}.$$

where c is the projected interval.

A sign convention for the product $KY\, q_b$ should be adopted here in order to avoid mistakes. The value $KY\, q_b$ is positive when both sides of angle w are ascending or descending to the vertex, otherwise it is negative.

The free edge, 8-22, of the groined vault cannot withstand any normal or tangential stresses, since there is no structural element which is able to resist them. Therefore, equating Eqs. 39 and 40 to zero and solving for T_x and T_y, the following is obtained:

$$T_x = -T \frac{\sin(\beta-\alpha)}{\sin \beta}, \quad \ldots\ldots\ldots 42$$

$$T_y = -T \frac{\sin \beta}{\sin(\beta-\alpha)} \quad \ldots\ldots\ldots 43$$

From equation 41, with w_b equal to 116 deg. and 34 minutes, angles for points 8-22 are found. These values are shown in column 12 of Table 2.

Using Eqs. 42 and 43, values of T_x and T_y are computed. These values are shown in columns 18 and 19 of Table 2.

Table 2. Stresses at the free edge.

Point	$\sqrt{\frac{(1+k^2x^2)}{(1+k^2y^2)}}$ 1	q_b 2	q^2_b 3	$1+q_b^2$ 4	$\sqrt{\frac{(1+k_2^2y^2)}{(1+k_2^2)}}$ 5	$KY.q_b$ 6	$KY.q_b+\cos w_b$ 7
8	1.1161	0.0000	0.0000	1.0000	1.0550	0.0000	-0.4472
9	1.1135	0.0505	0.0026	1.0011	1.0722	-0.0197	-0.4669
10	1.1251	0.1635	0.0267	1.0125	1.1053	-0.0716	-0.5188
11	1.1266	0.2726	0.0743	1.0365	1.1505	-0.1327	-0.5799
12	1.1433	0.3816	0.1456	1.0703	1.2116	-0.2043	-0.6515
13	1.1626	0.4906	0.2407	1.1141	1.2901	-0.2865	-0.7338
14	1.1834	0.5997	0.3596	1.1656	1.3766	-0.3794	-0.8266
15	1.2090	0.7087	0.5022	1.2257	1.4819	-0.4829	-0.9301
16	1.2375	0.8177	0.6686	1.2916	1.5951	-0.5970	-1.0442
17	1.2681	0.9267	0.8588	1.3634	1.7220	-0.7217	-1.1689
18	1.3120	1.0358	1.0729	1.4397	1.8702	-0.8570	-1.3042
19	1.3499	1.1448	1.3106	1.5201	2.0217	-1.0030	-1.4502
20	1.3994	1.2538	1.5720	1.6037	2.1810	-1.1595	-1.6067
21	1.4522	1.3628	1.8572	1.6905	2.3582	-1.3267	-1.7739
22	1.5868	1.4583	2.1266	1.7683	2.6029	-1.4905	-1.9377

Table 2. (Cont.)

Point	$K^2YX+\cos w$ 8	$\cos\alpha$ 9	$\cos\beta$ 10	Deg. Min. α 11	Deg. Min. β 12	Deg. Min. $\beta-\alpha$ 13	$\sin\beta$ 14
8	0.7160	0.6418	-0.4250	50-01	115-10	65-09	0.9001
9	0.7136	0.6400	-0.4398	50-12	116-06	65-54	0.8918
10	0.7065	0.6289	-0.4699	51-02	118-02	67-00	0.8749
11	0.6947	0.6166	-0.5040	51-56	120-20	68-34	0.8631
12	0.6781	0.5931	-0.5377	53-37	122-32	68-55	0.8431
13	0.6567	0.5648	-0.5688	55-37	124-40	69-03	0.8225
14	0.6307	0.5329	-0.5976	57-48	126-42	68-54	0.8018
15	0.5999	0.4962	-0.6276	60-15	128-52	68-37	0.7786
16	0.5644	0.4561	-0.6546	62-33	130-53	68-20	0.7560
17	0.5221	0.4117	-0.6788	65-41	130-45	67-04	0.7343
18	0.4791	0.3652	-0.6973	68-35	134-13	65-28	0.7167
19	0.4293	0.3180	-0.7173	71-49	135-50	64-01	0.6967
20	0.3748	0.2678	-0.7367	74-28	137-27	62-59	0.6762
21	0.3157	0.2173	-0.7522	77-27	138-47	61-20	0.6589
22	0.2517	0.1586	-0.7444	80-52	138-58	58-06	0.6565

Table 2. (Cont.)

Point	$\frac{\sin(\beta-\alpha)}{\sin\beta}$ 15	$\frac{\sin(\beta-\alpha)}{\sin\beta}$ 16	$\frac{\sin\beta}{\sin(\beta-\alpha)}$ 17	T_x k/ft. 18	T_y k/ft. 19	$\sqrt{\frac{1+k^2x^2}{1+k^2y^2}}$ 20
8	0.9074	1.0055	0.9979	-2.4655	-2.4588	1.0000
9	0.9128	1.0222	0.9780	-2.5222	-2.4158	0.9754
10	0.9205	1.0525	0.9501	-2.6452	-2.3855	0.9321
11	0.9308	1.0784	0.9273	-2.7928	-2.4015	0.9144
12	0.9331	1.1067	0.9035	-2.9449	-2.4042	0.8922
13	0.9339	1.1354	0.8807	-3.1322	-2.4296	0.8670
14	0.9329	1.1635	0.8595	-3.3433	-2.4698	0.8484
15	0.9312	1.1960	0.8361	-3.6106	-2.5241	0.8271
16	0.9294	1.2294	0.8134	-3.8849	-2.5703	0.8113
17	0.9210	1.2543	0.7973	-4.1895	-2.6631	0.7949
18	0.9097	1.2693	0.7878	-4.4439	-2.7582	0.7775
19	0.8989	1.2902	0.7751	-4.7607	-2.8600	0.7632
20	0.8909	1.3175	0.7590	-5.1103	-2.9440	0.7566
21	0.8774	1.3316	0.7510	-5.4135	-3.0531	0.7462
22	0.8489	1.2922	0.7745	-5.3626	-3.2142	0.7323

Table 2. (Concl.)

Point	$\sqrt{\frac{1+k^2y^2}{1+k^2x^2}}$ 21	V_x k/ft. 22	V_y k/ft. 23	ΔV_x k/ft. 24	ΔV_y k/ft. 25
8	1.0000	-2.4655	-2.4588	-3.8344	-3.8277
9	1.0299	-2.4661	-2.4811	-3.9112	-3.8304
10	1.0625	-2.4675	-2.5382	-4.0171	-3.8936
11	1.0936	-2.5537	-2.6263	-4.2051	-4.0290
12	1.1208	-2.6274	-2.6946	-4.3875	-4.1519
13	1.1534	-2.7156	-2.8023	-4.6613	-4.3473
14	1.1786	-2.8365	-2.9109	-4.9606	-4.5722
15	1.2090	-2.9863	-3.0516	-5.3136	-4.8629
16	1.2325	-3.1518	-3.1679	-5.6829	-5.1406
17	1.2580	-3.3300	-3.3502	-6.0952	-5.4182
18	1.2861	-3.4551	-3.5473	-6.3658	-5.9098
19	1.3103	-3.6334	-3.7475	-6.8669	-6.3274
20	1.3217	-3.8665	-3.8911	-7.3523	-6.7034
21	1.3400	-4.0395	-4.0911	-7.7597	-7.1524
22	1.3655	-3.9270	-4.3890	-7.7215	-7.7308

Step 4:

Using Eqs. 6 and 7, the values of V_x and V_y are found for points 8-22. These values are shown in columns 22 and 23 of Table 2.

The values of V_x and V_y shown in columns 33 and 34, Table 1 for points 8-22, are obtained on the assumption that $f_1(Y)$ and $f_2(X)$ are equal to zero. The stresses V_x and V_y, shown in columns 22 and 23 of Table 2, are obtained when T_b and S_b, the normal and tangential stresses, are set equal to zero. Therefore, to leave edge 8-22 completely free of stresses, a set of stresses ΔV_y and ΔV_x equal and opposite to the differences between the basic values V_x and V_y and the ones called V_x and V_y need to be assigned to the constants of integration, i. e.,

$$f_2(X) = \Delta V_y = V_y - V_y$$

$$f_1(Y) = \Delta V_x = V_x - V_x.$$

The computed values of ΔV_y and ΔV_x are shown in columns 24 and 25 of Table 2.

Step 6:

The stresses ΔV_x and ΔV_y introduced in step 5 disturb the equilibrium of the structure. Therefore, readjusting the stresses requires that the same stresses should be introduced at the groin. This can be accomplished by transferring ΔV_x and ΔV_y from the free end of each generator to the opposite ones, as if each generator were a tie or strut. Such transformation will produce, of course, alterations in the state of stresses at the interior points of the surface. However, these alterations are insignificant since the boundary points govern the design.

Accordingly, the stresses at the free edge 8-22, i. e., ΔV_x and ΔV_y are

transformed to the groin, points 22-42-1. The values obtained from this step are shown in columns 1 and 2 of Table 3.

Step 7:

The modified values of V_x and V_y at the groin, shown in columns 3 and 4, Table 3, are obtained by adding the basic values of V_x and V_y in columns 33 and 34 of Table 1 to those presented in columns 1 and 2 of Table 3.

Step 8:

Using Eqs. 6 and 7 the values of $T_{\overline{x}}$ and $T_{\overline{y}}$ are found for points 22-42-1. These values are shown in columns 7 and 8 of Table 3.

Step 9:

As in step 3, values of stresses along the other boundary line, 22-42-1, need to be investigated. This can be accomplished by using Eq. 41, with W_b equal to 71 deg. and 34 minutes in order to find the angle β for the points 22-42-1. Then, by using Eqs. 39 and 40, values of T_b and S_b can be obtained. The necessary computations for this step are shown in columns 9 to 41 of Table 3. Values of T_b and S_b are shown in columns 42 and 43 of Table 3.

Step 10:

Stresses T_b and S_b are stresses per unit length of edge. To obtain the forces concentrated at the points 22-42-1, i.e., FT_b and FS_b, these stresses must be multiplied by the corresponding real intervals. These intervals may be computed by the following formula:

$$I = \sqrt{(Z_i - Z_i + 1)^2 + C^2}$$

where

I = interval

C = the horizontal projection of the interval, i.e., 2.357.

the real interval = $I_r = \frac{I_i + I_i + 1}{2}$.

Table 3. Stresses at the groin.

Point	ΔV_x k/ft. 1	ΔV_y k/ft. 2	V_x k/ft. 3	V_y k/ft. 4	$\sqrt{\frac{1+k^2x^2}{1+k^2y^2}}$ 5	$\sqrt{\frac{1+k^2y^2}{1+k^2x^2}}$ 6	T_x k/ft. 7
22	-7.7215	-7.7308	-3.9270	-4.3890	0.7323	1.3655	-5.3623
23	-7.7597	-7.5380	-4.0274	-4.3882	0.7520	1.3298	-5.3556
24	-7.3523	-7.3452	-3.6580	-4.3096	0.7684	1.3014	-4.7605
25	-6.8669	-7.1524	-3.3164	-4.2848	0.7880	1.2690	-4.2085
26	-6.3658	-7.0028	-3.0833	-4.2542	0.7968	1.2551	-3.8698
27	-6.0952	-6.8531	-2.9880	-4.2399	0.8166	1.2246	-3.6591
28	-5.6829	-6.7034	-2.7486	-4.2168	0.8304	1.2043	-3.3101
29	-5.3136	-6.5781	-2.5466	-4.2171	0.8447	1.1838	-3.0147
30	-4.9606	-6.4527	-2.2726	-4.1318	0.8637	1.1578	-2.6312
31	-4.6613	-6.3274	-2.1918	-4.1933	0.8852	1.1297	-2.4761
32	-4.3875	-6.1882	-2.0762	-4.1586	0.8943	1.1182	-2.3216
33	-4.2051	-6.0490	-2.0984	-4.1495	0.9036	1.0988	-2.3057
34	-4.0171	-5.9098	-1.9523	-4.0724	0.9266	1.0792	-2.1069
35	-3.9112	-5.7460	-2.0035	-4.0045	0.9402	1.0636	-2.1309
36	-3.8344	-5.5821	-1.9969	-3.9227	0.9524	1.0502	-2.0971
37	-3.9112	-5.4182	-2.2272	-3.8325	0.9644	1.0369	-2.3094
38	-4.0171	-5.3257	-2.4190	-3.7968	0.9728	1.0279	-2.4865
39	-4.2051	-5.2331	-2.6855	-3.4582	0.9833	1.0170	-2.7312
40	-4.3875	-5.1406	-2.9319	-3.7106	0.9901	1.0100	-2.9612
41	-4.6613	-5.0480	-3.2491	-3.6470	0.9970	1.0030	-3.2588
42	-4.9606	-4.9555	-3.5767	-3.4806	0.9980	1.0020	-3.5838
1	-5.3136	-4.8629	-3.9343	-3.4836	1.0000	1.0000	-3.9343

Table 3. (Cont.)

Point	$Ty_{k/ft.}$	$\sqrt{\frac{(1+k^2x^2)}{(1+k^2y^2)}}$	q_h	KYq_b	q_b^2	$1+q_b^2$	$\sqrt{\frac{(1+k^2y^2)}{(1+q_b^2)}}$
	8	9	10	11	12	13	14
22	-2.8757	1.5868	0.7611	-0.7756	0.5715	1.2512	1.8457
23	-3.2999	1.4634	0.7499	-0.7289	0.5602	1.2499	1.7411
24	-3.3115	1.4212	0.7345	-0.6775	0.5399	1.2400	1.6892
25	-3.3764	1.3752	0.6725	-0.5890	0.4523	1.2021	1.6045
26	-3.3897	1.3445	0.6700	-0.5549	0.4489	1.2008	1.5588
27	-3.4623	1.3067	0.5650	-0.4398	0.3202	1.1496	1.4526
28	-3.5016	1.2727	0.5632	-0.4117	0.3160	1.1424	1.4148
29	-3.5622	1.2389	0.5124	-0.3485	0.2628	1.1269	1.3647
30	-3.5686	1.2046	0.4785	-0.3024	0.2297	1.1086	1.3099
31	-3.7119	1.1707	0.4546	-0.2645	0.2063	1.0979	1.2626
32	-3.7190	1.1520	0.4072	-0.2207	0.1678	1.0807	1.2266
33	-3.7495	1.1253	0.3621	-0.1761	0.1316	1.0641	1.1833
34	-3.7735	1.1001	0.3311	-0.1451	0.1096	1.0534	1.1482
35	-3.7650	1.0785	0.2900	-0.1135	0.0841	1.0438	1.1179
36	-3.7359	1.0612	0.2497	-0.0848	0.0623	1.0327	1.0916
37	-3.6961	1.0431	0.2160	-0.0646	0.4660	1.0212	1.0620
38	-3.6935	1.0320	0.1751	-0.0426	0.0306	1.0158	1.0463
39	-3.4000	1.0190	0.1362	-0.0267	0.0185	1.0092	1.0274
40	-3.6739	1.0100	0.0980	-0.0145	0.0096	1.0048	1.0148
41	-3.6361	1.0030	0.0597	-0.0058	0.0034	1.0019	1.0049
42	-3.4736	1.0020	0.0192	-0.0009	0.0037	1.0018	1.0038
1	-3.4806	1.0000	0.0000	-0.0000	0.0000	1.0000	1.0000

Table 3. (Cont.)

Point	$\hat{K}^2_{XY}\cdot\cos w$ 15	$\frac{KY_q}{y_b}\cdot\cos w_b$ 16	$\cos\alpha$ 17	$\cos\beta$ 18	Deg. Min. α 19	Deg. Min. β 20	Deg. Min. $\beta-\alpha$ 21
22	0.2517	-0.4584	0.1586	-0.2485	80-52	104-24	23-32
23	0.2835	-0.4127	0.1937	-0.2368	78-50	103-42	24-52
24	0.3133	-0.3613	0.2204	-0.2139	77-16	102-21	25-05
25	0.3459	-0.2728	0.2515	-0.1700	75-26	99-48	24-22
26	0.3713	-0.2387	0.2762	-0.1532	73-57	98-49	24-52
27	0.3989	-0.1236	0.3053	-0.0850	72-13	94-53	22-40
28	0.4220	-0.0955	0.3316	-0.0675	70-38	93-51	23-13
29	0.4447	-0.0323	0.3589	-0.0236	68-58	91-21	22-23
30	0.4659	0.0138	0.3868	0.0105	67-14	89-24	22-10
31	0.4849	0.0517	0.4142	0.0409	65-32	87-39	22-07
32	0.5034	0.0955	0.4370	0.0780	64-05	85-32	21-27
33	0.5202	0.1401	0.4623	0.1181	62-28	83-13	20-45
34	0.5351	0.1711	0.4860	0.1492	60-55	81-25	20-30
35	0.5487	0.2027	0.5088	0.1820	59-25	79-30	20-05
36	0.5606	0.2314	0.5283	0.2115	58-07	77-47	19-40
37	0.5712	0.2516	0.5476	0.2368	56-48	76-18	19-30
38	0.5797	0.2735	0.5617	0.2617	55-50	74-50	19-00
39	0.5870	0.2895	0.5761	0.2820	54-49	73-37	18-48
40	0.5926	0.3017	0.5867	0.2965	54-04	72-47	18-43
41	0.5966	0.3104	0.5948	0.3091	53-30	72-00	18-30
42	0.5992	0.3153	0.5980	0.3138	53-16	71-43	18-27
1	0.5999	0.3162	0.5999	0.3162	53-08	71-34	18-26

Table 3. (Cont.)

Point	Deg. Min. 2β 29	Deg. Min. $2\beta-\alpha$ 30	$\sin\alpha$ 31	$\sin\beta$ 32	$\sin^2\beta$ 33	$\sin(\beta-\alpha)$ 34	$\sin^2(\beta-\alpha)$ 35
22	208-48	127-56	0.9873	0.9686	0.9378	0.3966	0.1572
23	207-24	128-34	0.9811	0.9716	0.9442	0.4205	0.1768
24	204-42	127-26	0.9754	0.9769	0.9545	0.4239	0.1796
25	199-36	125-39	0.9679	0.9854	0.9712	0.4126	0.1701
26	197-38	124-41	0.9610	0.9882	0.9762	0.4205	0.1768
27	189-46	117-33	0.9522	0.9964	0.9910	0.3854	0.1485
28	187-42	116-04	0.9434	0.9977	0.9950	0.3942	0.1553
29	182-42	113-44	0.9334	0.9997	0.9990	0.3808	0.1451
30	178-48	111-34	0.9221	0.9999	0.9999	0.3773	0.1426
31	175-18	109-46	0.9102	0.9992	0.9980	0.3765	0.1416
32	171-04	106-59	0.8994	0.9970	0.9940	0.3657	0.1337
33	166-26	103-58	0.8867	0.9930	0.9860	0.3543	0.1258
34	162-50	101-55	0.8739	0.9888	0.9781	0.3502	0.1226
35	159-00	99-35	0.8609	0.9832	0.9668	0.3434	0.1179
36	155-34	96-27	0.8491	0.9773	0.9547	0.3366	0.1132
37	152-36	95-48	0.8368	0.9715	0.9418	0.3338	0.1111
38	149-40	93-50	0.8274	0.9652	0.9316	0.3256	0.1059
39	147-14	92-25	0.8173	0.9594	0.9200	0.3223	0.1037
40	145-34	91-30	0.8077	0.9552	0.9124	0.3209	0.1030
41	144-00	90-30	0.8039	0.9511	0.9045	0.3173	0.1008
42	143-26	90-10	0.8014	0.9495	0.9015	0.3165	0.0999
1	143-08	90-00	0.8000	0.9487	0.8999	0.3162	0.0998

Table 3. (Cont.)

Point	$\sin(2\beta-\alpha)$ 22	$\sin\beta\sin(\beta-\alpha)$ 23	$\sin\beta\cos\beta$ 24	$\cos(\beta-\alpha)$ 25	$\frac{\sin(\beta-\alpha)}{\cos(\beta-\alpha)}\times$ 26	$\pi\sin^2\beta$ 27	$\frac{2T\sin\beta}{\sin(\beta-\alpha)}$ 28
22	0.7887	0.3840	-0.2328	0.9168	0.3640	-5.0452	3.1853
23	0.7819	0.4105	-0.2304	0.9073	0.3819	-5.0563	3.4000
24	0.7941	0.4042	-0.2086	0.9057	0.3835	-4.5450	3.1449
25	0.8126	0.4001	-0.1673	0.9110	0.3759	-4.0890	3.0685
26	0.8223	0.4155	-0.1517	0.9073	0.3818	-3.7800	3.0943
27	0.8866	0.3819	-0.0861	0.9228	0.3576	-3.6206	2.7300
28	0.8983	0.3922	-0.0673	0.9190	0.3537	-3.2987	2.7086
29	0.9154	0.3800	-0.0235	0.9247	0.3520	-3.0095	2.5207
30	0.9300	0.3771	0.0104	0.9261	0.3494	-2.6310	2.5144
31	0.9411	0.3762	0.0408	0.9264	0.3487	-2.4750	2.3200
32	0.9564	0.3643	0.0776	0.9307	0.3400	-2.3856	2.1805
33	0.9704	0.3518	0.1172	0.9351	0.3318	-2.3705	1.9694
34	0.9784	0.3458	0.1474	0.9367	0.3279	-2.0764	1.9109
35	0.9860	0.3369	0.1789	0.9392	0.3220	-2.0673	1.8087
36	0.9937	0.3286	0.2061	0.9417	0.3169	-2.0000	1.7069
37	0.9949	0.3240	0.2300	0.9426	0.3142	-2.2452	1.6351
38	0.9978	0.3142	0.2520	0.9455	0.3075	-2.3188	1.5400
39	0.9991	0.3085	0.2705	0.9466	0.3045	-2.5186	1.4802
40	0.9997	0.3066	0.2834	0.9471	0.3042	-2.6999	1.4406
41	0.9999	0.3017	0.2840	0.9483	0.3008	-2.9398	1.4000
42	1.0000	0.3000	0.2977	0.9486	0.3003	-3.2216	1.3800
1	1.0000	0.2999	0.3000	0.9487	0.3000	-3.5377	1.3787

Table 3. (Concl.)

Point	$T_y \sin^2(\beta-\alpha)$ 36	$T_x \sin\beta \cos\beta$ 37	$T \sin(2\beta-\alpha)$ 38	$T_{\bar{y}} \sin(\beta-\alpha)\cos(\beta-\alpha)$ 39	$T_b \sin\alpha$ 40	$S_b \sin\alpha$ 41	T_{b_k}/ft. 42	S_{b_k}/ft. 43
22	-0.4519	1.2495	3.2745	-1.0495	-2.3118	-4.4750	-2.3400	-3.5350
23	-0.5189	1.2495	3.2365	-1.2218	-2.1752	-3.2642	-2.2131	-3.3365
24	-0.5948	0.9947	3.0873	-1.2699	-1.9949	-2.8121	-2.0453	-2.8800
25	-0.5745	0.7050	3.1186	-1.2656	-1.5950	-2.5580	-1.6499	-2.6402
26	-0.6000	0.5862	3.0599	-1.2915	-1.2857	-2.3546	-1.3385	-2.4475
27	-0.5145	0.3148	3.1700	-1.2387	-1.4051	-2.2461	-1.4750	-2.3604
28	-0.5446	0.2226	3.1035	-1.2389	-1.1347	-2.0872	-1.4301	-2.2186
29	-0.5158	0.0766	3.0400	-1.2517	-1.0046	-1.8649	-1.0712	-2.0000
30	-0.5056	-0.0263	3.0994	-1.2463	-0.6222	-1.8268	-0.6755	-1.9800
31	-0.5253	-0.1011	2.9032	-1.2937	-0.6803	-1.5084	-0.7476	-1.6524
32	-0.4956	-0.1802	2.8463	-1.2613	-0.7007	-1.4048	-0.7800	-1.5618
33	-0.4717	-0.2706	2.7251	-1.2316	-0.6728	-1.2229	-0.9849	-1.3791
34	-0.4600	-0.3099	2.7096	-1.2320	-0.6255	-1.1677	-0.7175	-1.3385
35	-0.4425	-0.3809	2.6400	-1.2111	-0.6211	-1.0480	-0.7219	-1.3300
36	-0.4232	-0.4322	2.5750	-1.1815	-0.7163	-0.9613	-0.8450	-1.1322
37	-0.4108	-0.5318	2.5000	-1.1600	-1.0209	-0.8082	-1.2199	-0.9665
38	-0.3910	-0.6251	2.4500	-1.1312	-1.1698	-0.6937	-1.4115	-0.8375
39	-0.3528	-0.7385	2.4000	-1.0335	-1.3912	-0.6280	-1.7023	-0.7700
40	-0.3780	-0.8375	2.3500	-1.1188	-1.6373	-0.3937	-2.0280	-0.4865
41	-0.3659	-0.9249	2.3199	-1.0916	-1.9057	-0.3034	-2.3800	-0.3790
42	-0.3468	-1.0654	2.3000	-1.0420	-2.1884	-0.1926	-2.7396	-0.2408
1	-0.3472	-1.1800	2.2988	-1.0420	-2.4062	-0.0768	-2.5600	-0.0960

These real intervals are shown in column 4 of Table 4. Values of FT_b and FS_b are shown in columns 5 and 6 of Table 4.

Step 11:

Forces FS_b are acting along the parabola 22-42-1. Therefore, their vertical components can be obtained by the formula

$$FS_b \sin\gamma = FVS_b$$

where

$$\sin\gamma = \frac{z_i - z_{i+1}}{I}.$$

I is as defined in step 10.

The horizontal component may be obtained by

$$FS_b \cos\gamma = FHS_b$$

where

$$\cos\gamma = \frac{2.357}{I}$$

Values of $\sin\gamma$, $\cos\gamma$, FHS_b, and FVS_b are shown in columns 7, 8, 20 and 21 of Table 4, respectively. FVS_b is considered positive when directed downward, and FHS_b is positive when directed from 1 to 22.

Step 12:

Forces FT_b are acting along the normal plane at the corresponding points of the parabola 22-42-1. But being membrane forces, they must be contained in the plane tangent to the hyper at the points. Therefore, they are acting along the intersections of the plane normal and tangent to the parabola 22-42-1 at each point.

By the use of calculus it can be shown that the direction cosine of the normal to a plane tangent to a certain surface is given by

Table 4. Forces.

Point	$Z_i - Z_{i+1}$ 1	$(Z_i - Z_{i+1})^2$ 2	Interval ft. 3	Real Interval ft. 4	$FT_{b\ k.}$ 5	$FS_{b\ k.}$ 6	$\sin\theta$ 7
22	1.7956	3.2242	2.9648	1.4824	-3.4688	-5.1895	0.6065
23	1.7614	3.1025	2.9411	2.9529	-6.5350	-9.8523	0.5999
24	1.7246	2.9742	2.9206	2.9308	-5.9944	-8.4407	0.5885
25	1.5803	2.4973	2.8373	2.8789	-4.7495	-7.6009	0.5558
26	1.5730	2.4643	2.8320	2.8346	-3.7941	-6.9377	0.5551
27	1.3291	1.7655	2.7055	2.7688	-4.0840	-6.5355	0.4905
28	1.3233	1.7600	2.7037	2.7046	-3.8678	-5.9964	0.4900
29	1.2058	1.4586	2.6476	2.6756	-2.8661	-5.3512	0.4548
30	1.1241	1.2658	2.6115	2.6295	-1.7562	-5.2064	0.4318
31	1.0682	1.1400	2.5884	2.5999	-1.9438	-4.2962	0.4152
32	0.9591	0.9187	2.5436	2.5660	-2.0015	-4.0072	0.3775
33	0.8536	0.7286	2.5600	2.5518	-2.5133	-3.5192	0.3333
34	0.7775	0.5451	2.4698	2.5149	-1.8044	-3.3662	0.3148
35	0.6825	0.4658	2.4536	2.4617	-1.7771	-3.2741	0.2890
36	0.5660	0.3434	2.4289	2.4412	-2.0600	-2.8656	0.2417
37	0.5071	0.2571	2.4104	2.4196	-2.8134	-2.2425	0.2105
38	0.4126	0.1704	2.3917	2.4010	-3.3900	-2.0213	0.1727
39	0.3216	0.1034	2.3790	2.3853	-4.0496	-1.8375	0.1350
40	0.2288	0.0512	2.3685	2.3737	-4.8007	-1.1521	0.0967
41	0.1405	0.0196	2.3601	2.3643	-5.6225	-0.8955	0.0831
42	0.0453	0.0021	2.3579	2.3590	-6.4516	-0.5680	0.0892
1	0.0000	0.0000	2.3570	1.1785	-3.1879	-0.1130	0.0000

Table 4. (Cont.)

Point	$\cos\gamma$ 8	$\cos\rho$ 9	Deg. Min. ρ 10	$\tan\rho$ 11	$\cos\epsilon$ 12	Dec. Min. ϵ 13	$\sin\epsilon$ 14
22	0.7935	-0.6642	131-37	-1.1257	0.6835	46-53	0.7300
23	0.8000	-0.6986	134-19	-1.0241	0.6198	51-42	0.7848
24	0.8055	-0.7158	135-43	-0.9753	0.5747	54-55	0.8183
25	0.8309	-0.7350	137-18	-0.9228	0.5108	59-17	0.8597
26	0.8320	-0.7547	138-00	-0.8693	0.4822	61-10	0.8760
27	0.8705	-0.7750	140-48	-0.8156	0.4000	66-25	0.9165
28	0.8705	-0.7945	142-37	-0.7641	0.3740	68-02	0.9274
29	0.8895	-0.8148	144-34	-0.7115	0.3226	71-12	0.9466
30	0.9006	-0.8321	146-19	-0.6665	0.2879	73-16	0.9577
31	0.9091	-0.8540	148-39	-0.6092	0.2534	75-19	0.9673
32	0.9250	-0.8725	150-45	-0.5600	0.2119	77-46	0.9773
33	0.9200	-0.8908	152-59	-0.5099	0.1700	80-13	0.9855
34	0.9235	-0.9048	154-48	-0.4706	0.1481	81-29	0.9890
35	0.9600	-0.9250	157-40	-0.4106	0.1166	83-11	0.9929
36	0.9696	-0.9405	160-08	-0.3613	0.0872	84-00	0.9945
37	0.9775	-0.9556	162-52	-0.3085	0.0646	86-18	0.9979
38	0.9850	-0.9685	165-35	-0.2571	0.0444	87-27	0.9990
39	0.9890	-0.9796	168-25	-0.2050	0.0267	88-28	0.9996
40	0.9894	-0.9899	171-51	-0.1432	0.0138	89-12	0.9999
41	0.9985	-0.9945	173-00	-0.1050	0.0087	89-30	0.9999
42	1.0000	-0.9999	179-11	-0.0143	0.0001	90-00	1.0000
1	1.0000	-1.0000	180-00	-0.0000	0.0000	90-00	1.0000

Table 4. (Cont.)

Point	$\sin \rho$	FVI_b k.	FRT_b k.	FNT_b k.	FHT_b k.	FHS_b k.	FVS_b k.
	15	16	17	18	19	20	21
22	0.7474	2.5875	-2.3050	-1.6812	-1.5711	5.3158	4.0750
23	0.7155	4.6850	-4.5589	-3.5750	-2.8203	7.8950	5.9000
24	0.6982	4.1892	-4.3048	-3.5208	-2.4779	6.7855	4.9513
25	0.6782	3.2206	-3.4985	-3.0064	-1.7821	6.3056	4.2250
26	0.6561	2.5043	-2.8599	-2.5087	-1.3723	5.7552	3.8474
27	0.6320	2.5852	-3.1647	-2.9000	-1.2659	5.6951	3.2011
28	0.6071	2.3478	-3.0685	-2.8486	-1.1498	5.2019	2.8375
29	0.5798	1.6588	-2.3542	-2.2274	-0.7567	4.7505	2.4296
30	0.5546	0.9746	-1.4611	-1.4056	-0.4255	4.6856	2.2401
31	0.5203	1.0105	-1.6598	-1.6022	-0.4150	3.9000	1.7815
32	0.4886	0.9772	-1.7450	-1.7053	-0.3682	3.9000	1.3100
33	0.4543	1.1140	-2.2400	-2.2252	-0.3810	3.2386	1.1710
34	0.4258	0.7687	-1.6293	-1.6091	-0.2418	3.1008	1.0603
35	0.3800	0.6755	-1.6422	-1.6324	-0.1950	3.1383	0.9455
36	0.3398	0.7000	-1.9375	-1.9282	-0.1690	2.7808	0.6899
37	0.2946	0.8300	-2.6806	-2.5700	-0.1662	2.1974	0.4725
38	0.2490	0.8440	-3.2800	-3.2750	-0.1458	1.9892	0.3483
39	0.2008	0.8099	-3.9653	-3.9635	-0.1058	1.8113	0.2478
40	0.1418	0.6816	-4.7498	-4.7498	-0.0655	1.1417	0.1113
41	0.1045	0.5865	-5.6057	-5.6057	-0.0560	0.8897	0.0744
42	0.0143	0.0925	-6.4516	-6.4516	-0.0064	0.5680	0.0496
1	0.0000	0.0000	-3.1879	-3.1879	-0.0000	0.1130	0.0000

Table 4. (Concl.)

Point	FH k_{22}	FV k_{23}
22	3.7447	6.6625
23	5.0747	10.5850
24	4.3076	9.1405
25	4.5235	7.4456
26	4.3829	6.3517
27	4.4292	5.7863
28	4.0521	5.1853
29	3.9938	4.0884
30	4.2601	3.2147
31	3.4850	2.7920
32	3.5318	2.2872
33	2.8576	2.2850
34	2.8590	1.7290
35	2.9433	1.6210
36	2.6118	1.3699
37	2.0312	1.3025
38	1.8434	1.1923
39	1.7055	1.0577
40	1.0762	0.7929
41	0.8337	0.6609
42	0.5616	0.1421
1	0.1130	0.0000

$$\cos\rho = \left[\frac{-1}{\sqrt{\left(\frac{\partial z}{\partial y}\right)^2 + \left(\frac{\partial z}{\partial x}\right)^2 + (-1)^2}}\right]$$

where

ρ is the angle between the normal and the positive direction of the Z-axis.

This normal to the tangent is also normal to the direction of the force FT_b which is contained in the tangent plane. Therefore, the forces FT_b make an angle $180-\rho$ with the XY-plane.

The vertical components of FT_b can be obtained, therefore, by

$$FVT_b = FT_b \sin(180-\rho) = FT_b \sin\rho$$

The projected components of FT_b on the XY-plane are equal to

$$FRT_b = FT_b \cos(180-\rho) = -FT_b \cos\rho$$

Forces FRT_b are not perpendicular to the projection of the groin 22-42-1. The angle of inclination of these forces with the projection of the groin can be obtained from Fig. 9. From this figure it can be shown that

$$a^2 + b^2 = l^2$$

and

$$e^2 = l^2 - (Z_2 - Z_1)^2$$

also,

$$\tan\gamma = \frac{Z_1}{b} \qquad \tan\rho = \frac{Z_2}{c}$$

$$\cos\gamma = \frac{d}{b} \qquad \cos\rho = \frac{c}{a}$$

Therefore,

$$e^2 = a^2 + b^2 - (c\tan\rho - b\tan\gamma)^2$$

but

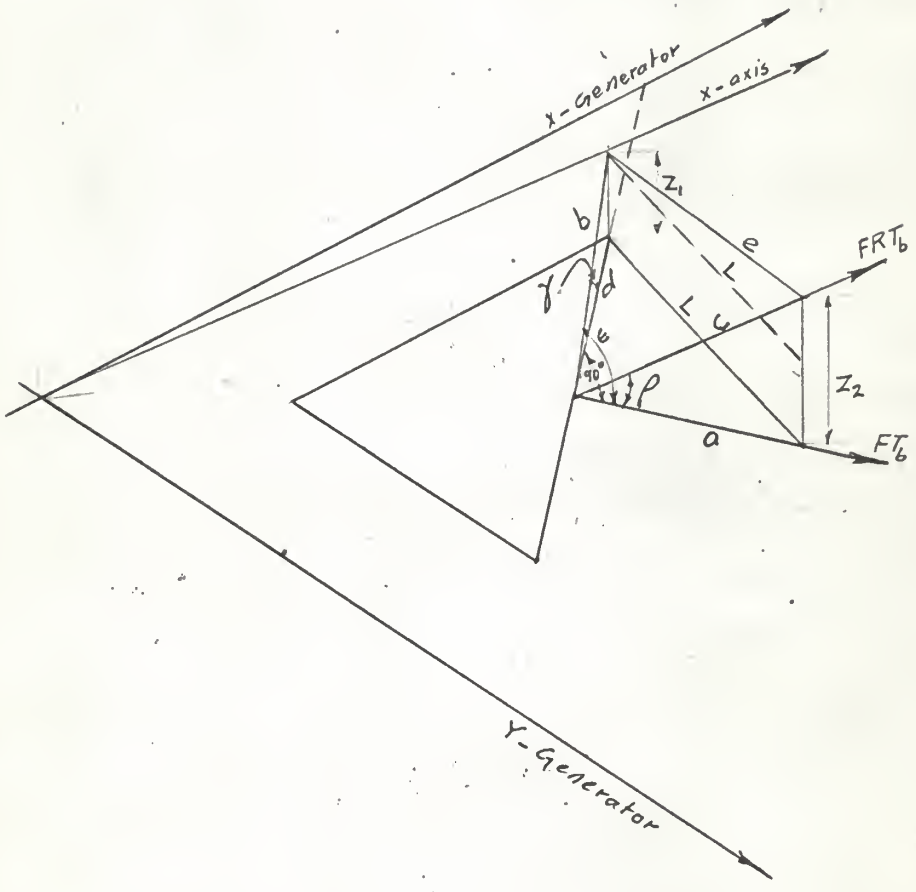

Fig.9- ANGLE ϵ.

$$e^2 = c^2 + b^2 - 2cb\cos\epsilon.$$

Therefore,

$$e^2 + b^2 - (c\tan\rho - b\tan\gamma)^2 = c^2 + b^2 - 2cb\cos\epsilon.$$

From which one can obtain

$$\cos\epsilon = -\tan\gamma\tan\rho$$

where

γ and ρ are the angles defined in steps 11 and 12.

When the angles ϵ are obtained, the forces FRT_b can be resolved into two components. These are normal to the projection of the groin, i.e., $FNT_b = FRT_b \times \sin\epsilon$ and the components tangential to the projection of the groin, i.e., $FHT_b = FRT_b \times \cos\epsilon$. These normal components are balanced by the normal components of the adjacent hyper.

Values of $\tan\rho$, $\cos\epsilon$, ϵ, $\sin\epsilon$, FVT_b, FRT_b, FNT_b and FHT_b are shown in columns 11, 12, 13, 14, 16, 17, 18 and 19 of Table 4, respectively.

Step 13:

The live load is usually assumed to be uniformly distributed on a horizontal projection. Therefore, in calculating the stresses due to this type of loading, Eqs. 30, 31 and 32 may be used. This implies that a method similar to that used in steps 1 to 11 in calculating the stresses due to dead load should be followed. However, the specified live load for roofs on a horizontal projection can be reduced to a surface load since an accurate calculation of the curved surface is possible. This surface area can be obtained by dividing the total vertical forces contributed to the groin, and shown in column 23, by the dead load per unit area, i.e.,

$$\text{surface area} = \frac{75.712}{0.05} = 1514.25 \text{ sq. ft.}$$

Assuming the L. L. to be equal to 30 lb. per sq. ft., the ratio of actual surface to the horizontal projection is

$$\frac{1514.25}{612.5} = 2.472.$$

The L. L. per unit surface area is then

$$W_L = \frac{30}{2.472} = 12.15 \text{ lb. per sq. ft.}$$

The ratio of L. L. to D. L. is

$$\frac{\text{L. L.}}{\text{D. L.}} = \frac{12.15}{50.00} = 0.243.$$

To include the effect of L. L., the values of stresses and forces obtained in the previous steps should be multiplied by 1.243.

Step 14:

Values of the horizontal and vertical components of forces at each point of the groin are shown in columns 22 and 23 of Table 4. If these values are multiplied by 2 x 1.243 (in order to include the forces contributed to the groin from the adjacent panel and the effect of live load), the total forces acting on the groin will be obtained.

After all the forces acting on the groin are obtained, it can be designed as a three-hinged or a two-hinged arch. The effective width acting as an arch, as recommended by the Portland Cement Association[8], is equal to $1.52\sqrt{rt}$, in which r is the average radius of the arch at the point of intersection of the adjacent hyper. However, the design of the arch is omitted since the main purpose of this report is to design the shell part of the structure.

Step 15:

Directions of principal stresses can be determined by letting S_b in Eq. 40 be equal to zero. Therefore,

$$\tan 2\beta = \frac{2T \sin \alpha + T_y \sin 2\alpha}{T_x + 2T \cos \alpha + T_y \cos 2\alpha}$$

where β and $90-\beta$ in this case are the angles of principal stresses with the positive part of the X-generators passing by the point. Values of principal stresses are, therefore,

$$T_1 = T_x \frac{\sin^2 \beta}{\sin \alpha} + 2T \frac{\sin \beta \sin (\beta-\alpha)}{\sin \alpha} + T_y \frac{\sin^2 (\beta-\alpha)}{\sin \alpha}$$

$$T_2 = T_x \frac{\cos^2 \beta}{\sin \alpha} + 2T \frac{\cos \beta \cos (\beta-\alpha)}{\sin \alpha} + T_y \frac{\cos^2 (\beta-\alpha)}{\sin \alpha}.$$

For point 22 it is found that

$$T_x = -5.3623,\ T_y = 2.8757, \text{ and } T = 4.15.$$

Therefore,

$$\tan 2\beta = -1.08$$

and

$$\beta = 66^\circ\text{-}23'.$$

Then

$$\sin \beta = 0.9162,\ \cos \beta = 0.4006$$

$$\sin (\beta-\alpha) = 0.2501,\ \cos (\beta-\alpha) = 0.9682.$$

From this one can obtain

$$T_1 = 6.68 \text{ k/ft. compression}$$

$$T_2 = 0.36 \text{ k/ft. tension.}$$

Therefore,

$$fc' = \frac{6.68 \times 1.243}{12 \times 3} \times 1000 = 230 \text{ psi},$$

and

$$ft' = \frac{0.36 \times 1.243}{3 \times 12} \times 1000 = 12.43 \text{ psi}.$$

These values are well below the allowable limits specified by the Building Code (ACI 318-63).

By inspection of other values of T, T_x and T_y, shown in column 31 of Table 1 and columns 7 and 8 of Table 3, respectively, it is evident that no further checking is required.

The above stresses do not require any reinforcement. However, ACI Committee 334[11] stated that "Minimum reinforcement shall be provided as required in the Building Code (ACI 318-63) even where not required by analysis." This reinforcement is usually provided to accomodate unsymmetrical loads and stresses due to volumetric changes.

The minimum reinforcement specified in article 807 ACI 318-63 may be used in this case. Therefore,

Min As = 0.002 x 12 x 3 = 0.072 sq. in. per ft.

Using #3 at 12 in. c. to c. provides 0.11 sq. in. per ft.

It is desirable to place the reinforcement along the generators, so that such reinforcement runs along straight lines.

Discussion of Results

As anticipated, it is evident from the results obtained in step 15 of the design for the groined vault that the stresses in concrete are well below the allowable stresses specified by the ACI Building Code 318-63. However, the thickness of the shell is not usually dictated by the strength requirements but by the cover over the reinforcement, better insulation, and fire proofing. Therefore, it seems that there is no need to reduce the thickness of the shell.

An approximate check of the accuracy of the results can be obtained by comparing the real surface area of the triangle 1-8-42-1 to its projection on the XY-plane, as suggested by Candela[6], i.e.,

$$\frac{1514.25}{612.5} = 2.472.$$

This ratio seems to be reasonable, especially if it is compared to the ratio 2.8 obtained by Candela in his example of a groined vault 20 m. sq. in plan and with a rise of 10 m.

Conclusion

The membrane theory proves to be a satisfactory method to give a reasonable estimate of the stresses in hyperbolic paraboloid shells. With the provision that they are subjected to a uniformly distributed load, the boundary conditions satisfy the conditions of equilibrium, and the rise-to-span of shell ratio is within the specified limit of $\frac{1}{5}$.

The hyperbolic paraboloid shells have become very popular and widely favored because they are well-adapted to the use of concrete. They show a remarkable resistance to any form of vibrational shock. They are economical and also give the architect an opportunity to develop more imaginative and graceful shapes of structures than the conventional beam and column buildings.

Acknowledgment

Grateful acknowledgment is made to Professor V. H. Rosebraugh for efficient direction of the work, encouragement throughout the preparation of this report, and for aid in organizing the material.

THE STRESSES IN HYPERBOLIC PARABOLOID SHELLS USING THE MEMBRANE THEORY

by

Yousif Kellow Dawood

B.S., University of Baghdad, 1959

AN ABSTRACT OF
A MASTER'S REPORT

submitted in partial fulfillment of the

requirements for the degree

MASTER OF SCIENCE

Department of Civil Engineering

KANSAS STATE UNIVERSITY
Manhattan, Kansas

1965

AN ABSTRACT

The membrane theory in many cases gives a reasonable estimate of the stress distribution of doubly curved shells. With the provision that they are subjected to a uniformly distributed load, the boundary conditions satisfy the conditions of equilibrium, and the rise-to-span of shell ratio is not less than 1/5. It is a good by-pass method to avoid the elaborate calculations encountered in using the bending theory.

The hyperbolic paraboloid surface can be defined as a surface of translation formed by moving a vertical parabola, opened upward, over another vertical parabola opened downward. It can also be defined as a warped parallelogram formed by moving a straight line along two nonparallel, nonintersecting lines in space.

The equation Z=KXY represents the simplest possible equation of the second degree which describes the surface of the hyperbolic paraboloid.

The general equations for membrane stresses for doubly curved shells can be obtained by writing the expressions for the equilibrium of an element formed by four intersecting lines contained in the surface. The expressions for equilibrium can be simplified by transforming the actual stresses acting on the element into fictitious stresses acting on the projection of the element on the XY-plane. The resulting expressions are in the form of three partial differential equations of the second order. The use of the stress function will reduce these three equations to one. This will facilitate the solution of the differential equations. However, in the case of the hyperbolic paraboloid shells, subjected to a uniform surface load or uniformly distributed load on a horizontal projection, direct integration of the partial differential equations is relatively simple.

The hyperbolic paraboloid shells have become very popular and widely favored because they are well-adapted to the use of concrete. They show a remarkable resistance to any form of vibrational shock, are more economical, and also give the architect an opportunity to develop more imaginative and graceful shapes of structures than the conventional beam and column buildings.

The groined vault is taken as a design example. The basic stresses in the structures are found by using the equations of stresses previously derived. However, readjustment of stresses is required in this case due to the existence of a free edge which cannot withstand any types of stresses, since there is no structural element which is able to resist them. This readjustment includes cancelling out the stresses calculated at the free edge by introducing a set of stresses equal and opposite to those obtained at this edge. This involves the introduction of the same additional stresses at the groin. Furthermore, the horizontal and vertical components of forces contributed to the groin by the shell are calculated, and a suggested procedure for design of the groin is presented. The principal stresses are also obtained which are used as the basis of design for the concrete shell section.